

Advanced Power Saving Technologies for UHF Band Active RFID Systems

WEI Dacheng

A Thesis Submitted in Partial Fulfillment

of the Requirements for the Degree

of Master of Philosophy

in

Electronic Engineering

©The Chinese University of Hong Kong

September 2006

The Chinese University of Hong Kong holds the copyright of this thesis. Any person(s) intending to use a part or whole of the materials in the thesis in a proposed publication must seek copyright released from the Dean of the Graduate School.


Abstract of thesis entitled: **Advanced Power Saving Technologies
for UHF Active RFID Systems**

Submitted by **WEI, Dacheng**

For the degree of **Master of Philosophy**

Advanced Power Saving Technologies for UHF Band Active RFID Systems

ABSTRACT



In the past decades, millions of PCs are connected to a Network. Then tens of millions of mobile phones and other handhelds are all connected to a Network. Uncountable Network services such as data exchange, instant messaging and many more services are provided and make our life more and more convenient. But all these are just the beginning of our digital world. Soon, billions of devices will have their own digital numbers and connect to a network. Businesses will run more efficiently and consumers will experience better and more innovative services. All these incredible changes are based on an innovative technique—RFID.

Typically there are three kinds of RFID systems—Passive RFID, Semi-Passive RFID and Active RFID system. Each of them focuses on different applications. Active RFID systems mainly focus on applications which need long operating distance, large memory size and under harsh operating environment. In this

Advanced Power Saving Technologies for UHF Band Active RFID Systems



ABSTRACT

In the past decade, millions of RFID tags have been deployed in various applications. The number of active tags in a system is increasing rapidly. This has led to the development of advanced power saving technologies for UHF band active RFID systems. These technologies are designed to reduce the power consumption of the tags, thereby extending their battery life and reducing the overall system power consumption. This paper discusses the challenges associated with power saving in UHF band active RFID systems and presents a comprehensive survey of the state-of-the-art power saving techniques. The paper also discusses the trade-offs between power saving and other system performance metrics, such as read range and data rate. Finally, the paper concludes with some future research directions in this area.

dissertation, an Active RFID system is implemented for container yard management. This active RFID system is complied with ISO18000-7 which is currently the only Active RFID standard in the world. To save more power, a novel power saving scheme is proposed. Further more, this power saving scheme also has the capability to reduce the influence from other disturbing signals.

A novel EE shape antenna is proposed in this dissertation for an Active RFID system application. Measurement results show that this EE antenna does not be affected by a metallic background. The maximum antenna gain is 5.6 dBi which is a reasonable value for this application. A Lossy Transmission Line Model is used to explain the working mechanism of this antenna. To increase the bandwidth of the antenna, a V shape feeding structure is also proposed. A significant improvement of bandwidth can be achieved with the V shape structure. Moreover, the antenna gain does not be affected because of this V shape structure.

論文題目：UHF 頻段主動式射頻識別系統的省電技術研究

提交人 韋大成

提交學位 哲學碩士

UHF 頻段主動式射頻識別系統的省電技術研究

摘要：

在過去的二十年間，數以千萬計的電腦以網路的形式連接在一起，而後，越來越多的手持設備，如手機，PDA 也通過網路進行互連。大量豐富多樣的網路服務如即時資訊交換，大容量的資料傳輸令我們的生活變得越來越方便快捷。然而，這些都僅僅是我們未來數字生活的開始。在不遠的將來，每一件物品，大到一輛汽車，小到一包食品，都將擁有它們唯一的識別號並且連接到網路中。所有的這些令人難以自信的變化都是源于一項具有創新意義的新技術——射頻識別技術。

總的來說，目前世界上主要有三種射頻識別系統——被動式射頻識別系統，半被動式射頻識別系統和主動式射頻識別系統。這三種不同的系統所針對的應用領域各有不同。對於主動式射頻識別系統，它主要是針對了遠距離，大容量和相對較惡劣的工作環境的應用場合。在這片論文中，我們主要針對集裝箱管理開發了一套主動式射頻識別系統。該系統相容 ISO18000-7 協定。為了達到省電的目的，我們提出了一套新型的省電工作模式。這種工作模式同時也具備了原協議所不具備的抗干擾能力。

爲了適應集裝箱工作環境的需要，我們提出了一種新型的 EE 形天線。從測試的結果中我們可以清楚的看出，金屬背景對該天線的影響非常小。該天線的最大增益爲 5.6dBm. 相對於集裝箱管理應用該增益是一個比較合理的值。爲了分析該天線的工作原理，我們用損耗傳輸線模型來描述它的天線輸入特性。爲了提高天線的帶寬，我們採用一種 V 形結構。從實驗結果可以看出，在不影響天線增益的前提條件下，該結構極大的提高了天線的帶寬。

Acknowledgements

I would like to express my gratitude to my supervisor, Professor Li, for his patience and invaluable encouragement, guidance and support during the whole period of my study in the university.

I am also very grateful to my parents in the KFID group, especially Dr. Tingting Yu and Dr. Honggang Wang. In the past few years, I could also like to thank my colleagues, Mr. Hai Gu, Mr. Jing Wang, Mr. Xin Guo, Mr. Wei Niang, Mrs. Liang Li.

To my family

We have many interesting and exciting discussions and I learn a lot from them. Without their help, support and encouragement from their parents, I could never finish this thesis in a short time.

Finally, I am very grateful for my parents and my wife for their unconditional support and encouragement. I also bear my sincere thanks to my girlfriend because of her love and support without any complaint.

In all I say, every heart, thank you!

Acknowledgements

I would like to express my gratitude to my supervisor, Professor Ke-Li Wu for his patience and invaluable encouragement, guidance and support during the whole period of my study in the university.

I am also very grateful to everyone in the RFID group especially Dr. Yingzeng Yin and Dr. Hongyang Wang. I got lots of helps form them in the past few years. I would also like to thank to all my colleagues, Mr. Hai Hu, Mr. Ming Shen, Mr. Xin Gao, Mr. Wei Meng, Ms. Chetna, and Mr. Qinghua Li. We have many interesting and exiting discussions and I learn a lot from them. Without help, support, and encouragement from these persons, I would never have been able to finish this work.

Finally, I am very grateful for my parent and my sister. Their understanding, support and love encouraged me to work hard. I also give my sincere thanks to my girlfriend because of her love and support without any complaint or regret.

To all I say a very hearty "Thank You!"

TABLE OF CONTENTS

Sections	Pages
Table of Contents	VIII
List of Tables	XI
List of Figures	XII
List of Abbreviations	XV

Chapter 1 Introduction

1.1 Introduction to RFID system.....	1
1.2 Why we choose Active RFID system.....	4
1.3 Objective of the research.....	6
1.3.1 Requirement analysis.....	7
1.3.2 Selection of RFID system and standard.....	8
1.4 Original contribution of this dissertation.....	9
1.5 Organization of the dissertation.....	9
Reference	10

Chapter 2 Implementation of An Active RFID System

2.1 RFID System hardware design and related protocol.....	1
2.2 Introduction to ISO 18000-7.....	7
2.3 Microcontroller specification.....	12
2.4 RF model specifications.....	14

2.5	Communication between a PC and a Reader.....	15
2.6	Programming.....	16
2.6.1	Procedure sequences of Reader and Tag.....	17
2.6.2	Sequence of data transmission and reception.....	24
2.6.3	CRC implementation.....	28
2.7	Testing result.....	31
	Reference.....	35

Chapter 3 Novel Power Saving Methods for an Active RFID System

3.1	Some drawbacks of the existing Active RFID protocol.....	1
3.1.1	Power consumption problem.....	1
3.1.2	Multi-Reader problem.....	9
3.2	Solutions of the Multi-Reader problem and power saving problem.....	10
3.2.1	A solution to the power saving problem.....	11
3.2.2	A solution to the Multi-Reader problem.....	16
	Reference.....	21

Chapter 4 A Probe-fed Compact Half-wave Length Dipole Antenna for Active RFID System

4.1	Requirement of an antenna for Active RFID system.....	1
4.2	A probe-fed half-wave length dipole EE shape antenna for metallic object application.....	2

4.3 Electromagnetic simulation results.....	5
4.4 Operating principle analysis.....	9
4.5 Using V shape structure to increase the bandwidth.....	19
4.6 Prototyping and measurement results.....	22
4.7 Conclusion.....	28
Reference.....	29

Chapter 5 Conclusion

List of Tables

Numbers		Pages
Table 1.1	Comparison of different ID systems	1-3
Table 2.2.1	Reader to Tag Message Format	2-9
Table 2.2.2	Command Codes	2-9
Table 2.2.3	Broadcast response message format	2-9
Table 2.2.4	Point-to-Point response message format	2-10
Table 2.7.1	Static Current Consumption of a Tag	2-32
Table 2.7.2	Communication Distance Testing	2-33
Table 4.4.1	Basic Parameter of the Lossy Transmission Line	4-14
Table 4.5.1	Comparison between the Antennas with and without V Shape Structure	4-21

List of Figures

Numbers		Pages
Figure 1.2.1	Basic principle of Passive RFID	1-4
Figure 1.3.1.1	Container Types	1-7
Figure 2.1.1	Hardware Structure of Tag	2-1
Figure 2.1.2	Hardware Structure of a Reader	2-5
Figure 2.1.3	Whole System Block Diagram	2-6
Figure 2.2.1	Data Packet Format	2-8
Figure 2.2.2	Anti-collision between multiple tags and single reader	2-10
Figure 2.6.1.1	Working Sequence of Reader	2-18
Figure 2.6.1.2	Calibration for RX and TX mode	2-21
Figure 2.6.1.3	Point-to-Point Communication procedure of Reader	2-22
Figure 2.6.1.4	Wake Up Strategy	2-23
Figure 2.6.1.5	Operating Sequence of Tag	2-23
Figure 2.6.2.1	Data Packet Format	2-24
Figure 2.6.2.2	Manchester Encoding Data Stream	2-25
Figure 2.6.2.3	Data Transmission	2-26
Figure 2.7.1	Top View of a Tag	2-34
Figure 2.7.2	Bottom View of a Tag	2-34
Figure 2.7.3	Top View of a Reader	2-34
Figure 3.1.1.1	Wake up Sequence	3-2
Figure 3.1.2.1	Two Areas with Overlap	3-9

Figure 3.2.1.1	Time Sequence Diagram of the Modulated Time Marker	
	Wake-up Scheme	3-12
Figure 3.2.1.2	Comparison between Two Wake-up Scheme	3-14
Figure 3.2.1.3	Comparison between Two different Wake-up Schemes	
	under frequently operating of tags	3-15
Figure 3.2.2.1	TDMA Scheme	3-16
Figure 3.2.2.2	Reader Distribution Scheme	3-17
Figure 3.2.2.3	FDMA Scheme	3-19
Figure 4.2.1	EE Antenna Geometry and 3D View	4-4
Figure 4.3.1	Return Loss of EE Antenna	4-5
Figure 4.3.2	E Plane	4-6
Figure 4.3.3	Current Distribution of EE Antenna	4-8
Figure 4.4.1	EE Antenna without supporters and pads	4-9
Figure 4.4.2	Different Feeding Positions	4-11
Figure 4.4.3	S Parameters of the Antenna with Different	
	Feeding Point	4-12
Figure 4.4.4	Real Part of input impedance from Lossy	
	TLN Model	4-15
Figure 4.4.5	Imaginary Part of Input Impedance from	
	Lossy TLN Model	4-16
Figure 4.4.6	Real Part of Input Impedance from IE3D	4-16
Figure 4.4.7	Imaginary Part of Input Impedance form	

	IE3D	4-17
Figure 4.4.8	Imaginary Part with Feeding Pin Effect	4-18
Figure 4.4.9	Comparison of S parameter between IE3D and Lossy TLN Model	4-19
Figure 4.5.1	V Shape Structure Antenna	4-20
Figure 4.5.2	$ S_{11} $ of the V Shape Structure Antenna	4-21
Figure 4.6.1	Original EE Antenna	4-22
Figure 4.6.2	$ S_{11} $ of Original EE Antenna without V shape structure.	4-22
Figure 4.6.3	Original EE Antenna without Metallic Background	4-23
Figure 4.6.4	Original EE Antenna with Metallic Background	4-23
Figure 4.6.5	V Shape Structure Antenna	4-24
Figure 4.6.6	$ S_{11} $ of V Shape Structure Antenna With and Without Metallic Background	4-25
Figure 4.6.7	V Shape Antenna With Metallic Background	4-26
Figure 4.6.8	Comparison Result between Simulation and Experiment	4-26
Figure 4.6.9	Comparison between Original EE Antenna and a V Structure EE antenna	4-27

List of Abbreviations

RFID	Radio Frequency Identification
EPC	Electronic Product Code
ISO	International Organization for Standardization
GND	Ground
TLN	Transmission Line
RMS	Root Mean Square
NF	Noise Factor
BW	Bandwidth
AWGN	Additive White Gaussian Noise
GSM	Global System for Mobile Communications
TDMA	Time Division Multiple Access
SSMA	Spread Spectrum Multiple Access
FHMA	Frequency Hopped Multiple Access
CDMA	Code Division Multiple Access
FDMA	Frequency Division Multiple Access

CHAPTER

1

INTRODUCTION

1.1 Introduction to RFID system

With the rapid development of RFIC and the low power microprocessor technology, RFID technology has been becoming one of the most important technologies in the twenty-first century. RFID technology will be widely employed in our everyday life. The technology can be used in retail, warehouse management, tracking items, location, airport luggage management, supply chain, even home security for improving productivity and efficiency.

Among all applications, supply chain is the biggest beneficiary of RFID technology. A supply chain is complex. The core of supply chain is the management process. Usually the process includes three phases—Procurement, Purchasing, and Support [1]. These three phases involve customer business requirements, creation of a purchase order, the shipment of the finished goods, receipt of the finished goods, and so on. Every small goods in this complex supply chain should be tracked at every step of the process. We can image if all these small steps are recorded by

paper, how complex they will be. Even we use barcode to identify every small goods, the work load is still very heavy because all goods need to be scanned at least one time by hand and sometimes they need to be scanned several times because of the dust or spot on the surface of them.. Furthermore, from the size of barcode we know that the data density is low. One barcode can not carry a large data quantity. For a typical barcode its data quantity is 1~100 byte. For instance, UPC-A barcode is composed of 12 digits and EAN-13 is composed of 13 digits. This data size is not enough for every small item to have any detail description of their properties. From all these requirements we finally recognize that a new technology must be employed. RFID technology is developed for this kind of application and now it extends to many other regions.

There are many identification technologies. For instance, Optical character recognition, Biometric procedures, Voice identification, Fingerprinting procedures, Smart cards, Memory cards, and Microprocessor cards can all be used for identification. Table 1.1 shows the comparison [2] of these different technologies.

System parameter	Barcode	OCR	Voice Recog.	Biometry	Smart Card	RFID System
Typical data quantity(bytes)	1-100	1-100	–	–	16~64k	16~64k
Data density	Low	Low	High	High	Very high	Very high
Machine readability	Good	Good	Expensive	Expensive	Good	Good
Readability by People	Limited	Simple	Simple	Difficult	Impossible	Impossible
Influence of dirt/damp	Very high	Very high	–	–	Possible (contacts)	No influence

Influence of (opt.) covering	Total failure	Total failure	–	Possible	–	No influence
Influence of direction and position	Low	Low	–	–	Uni-directional	No influence
Degradation/wear	Limited	Limited	–	–	Contacts	No influence
Purchase cost/reading electronics	Very low	Medium	Very high	Very high	Low	Medium
Operating costs (e.g. printer)	Low	Low	None	None	Medium (contacts)	None
Unauthorized copying/modification	Slight	Slight	Possible	Impossible	Impossible	Impossible
Reading speed (including handling of data carrier)	Low ~4s	Low ~3s	Very low >5s	Very low >5-10s	Low ~4s	Very fast ~0.5s
Maximum distance between data carrier and reader	0~50cm	<1 cm	0~50cm	Direct contact	Direct contact	0~5m Microwave

Table 1.1 Comparison of different ID systems

1.2 Why we choose Active RFID system

Generally, there are two kinds of RFID systems—Passive RFID system and Active RFID system. They have different operating principles and applications. In order to replace barcode system, passive tags should be as cheap as possible. For a simplest Passive RFID system, it should include two main parts. One is passive tag another is reader. A passive tag does not need a battery. Its required energy is from a reader. The basic operating principle is shown in Figure 1.2.1

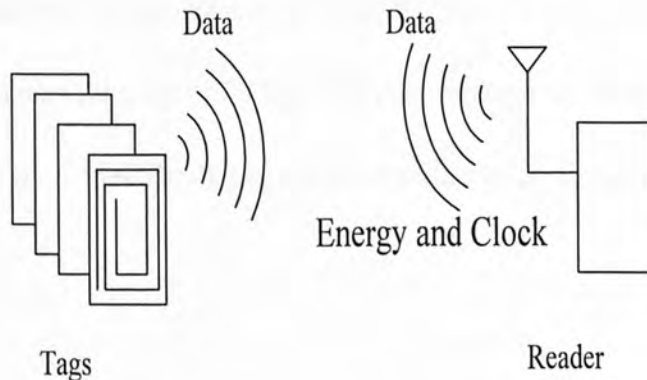


Figure 1.2.1 Basic principle of Passive RFID

Figure 1.2.1 is a basic passive RFID system. It involves Tags and Readers. A tag that is attached to the object to be identified is the actual data carrier device of an RFID system. Inside a passive tag there must include several main models—rectifier, clock extracting circuits, modulation and demodulation circuits, logic control circuits, coding and decoding circuits, memory, and antenna. All these circuits need power. The energy for these circuits is from Reader. When a reader

sends continuous wave to a tag, a rectifier inside tag will directly convert the continuous wave to DC. This DC current is the power source of all circuits in a tag. Firstly we try to find out why the operating distance of Passive RFID is so short.

Active RFID system is another kind of RFID system and it is more like a small communication system. It includes two main parts—Reader and Tag. The most significant character of Active RFID is that there is a battery inside an active tag. There is a transceiver inside every tag for long distance communications. An important issue in design an active RFID system is a power saving method. Another important issue is the cost of a tag. The performance of an active RFID tag will also be affected by a metallic background when a tag is directly attached to a metallic object.

Active RFID technology can be widely used only when these two issues are solved. Compared to a passive RFID system, the active RFID system has its own benefits [4]. First of all, the communication range of active RFID system is larger than passive RFID system. Secondly, the memory size of active RFID system is larger than passive RFID system. Further more the memory size of active RFID system is easily expanded and this is depended on different requirements. Thirdly, tags may be able to talk to other tags. This is very important in some applications. Using Tag-to-Tag communication can efficiently avoid blind area which is generated by blocking of EM wave. Fourthly, various sensors can be combined with tags to

monitor the environments around tags. This kind of application is useful for harmful gas monitor or preventing a forest fire. Sometimes battery can drive other functions such as GPS or a display. Thus how to save more power is the biggest issue of an active RFID system. Compared with passive RFID systems, the active tag is larger and more expensive.

From the above introduction we can understand that active RFID systems and passive RFID systems have different operating principle and focus on different applications. For short range applications we choose passive RFID systems. On the contrary, for long range and large memory applications we choose active RFID systems.

1.3 Objective of the research

The objective of the research has two fold: (1) developing effective and novel power saving technologies for active RFID systems, which will be superior than the method used proposed in ISO18000-7 protocol; and (2) a novel high gain antenna that is suitable for both metallic and non-metallic background applications.

1.3.1 Requirement analysis

Firstly, different containers have different status. Containers can separate into several types according to different goods [5].

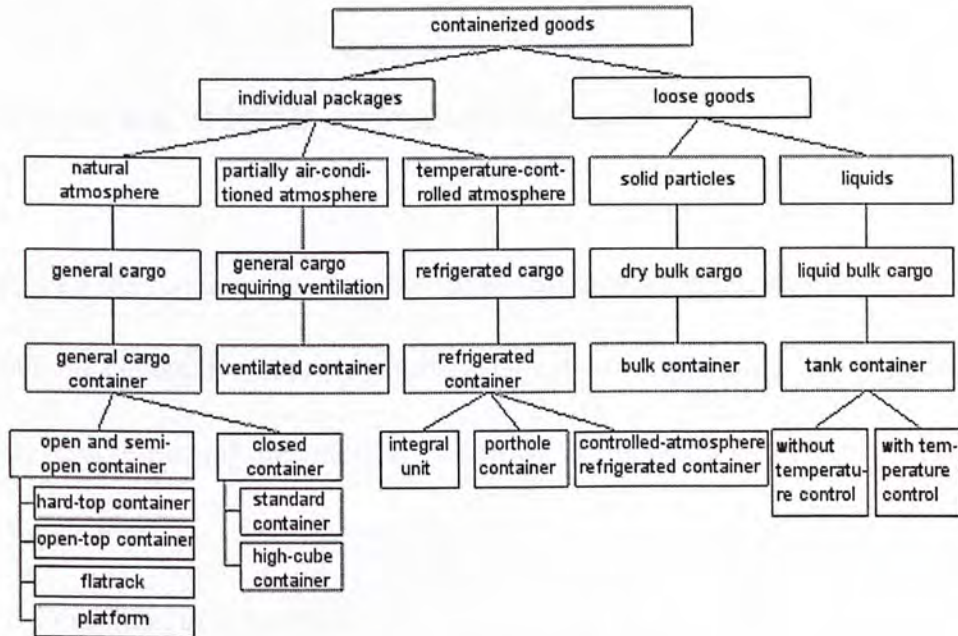


Figure 1.3.1.1 Container Types

Different types of container will be treated in different ways in a container yard. Thus we need a very detailed inventory list for every container and this inventory list can immediately update according to the change of goods. It means a large memory size is needed.

Secondly, the area of a large container yard is about 100,000 square meters. Usually there are 10,000 containers in a container yard. If every tag on a container need to be detected one by one using a hand-held reader, the work load will be too heavy. To cover this large area we need to develop a long distance, at least 100 meters, Read/Write RFID system and all tags should be identified automatically.

Thirdly, most of containers are made by metal. Thus tags should have the capability of working in a metallic environment. The reading or writing distance should not be affected by the metallic container.

1.3.2 Selection of RFID system and standard

To meet all the requirements of a container yard management, Active RFID system is a suitable choice. It can provide satisfied communication range and large memory size to reserve enough inventories. Following is the detail objective of our active RFID system:

1. Compliant to ISO 18000-7
2. Long communication distance up to 100 meters
3. Multi-reader and Multi-tag co-operation.
4. Large memory size (>50kByte) of tags.
5. A reader is controlled by a computer through RS232 port.
6. Ultra low power tag (a 2000mA battery can last 5 years).
7. EIRP \leq 6dBm
8. A high gain antenna is designed for non-metallic and metallic background applications.

1.4 Original contribution of this dissertation

A practical active RFID system including tags and readers is developed for container yard managements. Several power saving methods are proposed in this dissertation. Using these methods can significantly save power for an active tag without increasing the size or the cost of an active tag.

An EE shape antenna is proposed for the container yard application. This antenna will not be affected by the metallic background. A V shape feeding structure for increasing bandwidth is also proposed for this application. The bandwidth can be significantly increased with this V shape feeding configuration.

1.5 Organization of the dissertation

In Chapter 1, we introduce two different types of RFID systems. Some comparisons are given. From the comparison we can clearly find which type of RFID system is suitable for our applications. The implementation of an active RFID for container yard application is described in Chapter 2. In this chapter the whole system design and details of every part will be discussed. Several new power saving methods are proposed in Chapter 3. At the beginning of Chapter 3 we will discuss the disadvantage of existing protocols and then introduce the new power saving methods. In Chapter 4 we propose an EE shape antenna and its improvement. A mathematic model of the EE antenna will be also give to interpret the working

mechanism of the antenna. All simulation results and experiment results will be shown in the chapter. Conclusions of the research will be given in Chapter5.

Reference:

- [1] RFID Radio Frequency Identification
- [2] Klaus Finkenzeller, *RFID Handbook—Fundamentals and Applications in Contactless Smart Cards and Identification*, John Wiley & Sons 2003
- [3] *860MHz–930MHz Class I Radio Frequency Identification Tag Radio Frequency & Logical Communication Interface Specification Candidate Recommendation, Version 1.0.1*
- [4] Peter Harrop, *Active RFID and its Big Future*. IDTech Ltd
- [5] German transport insurers' loss prevention committee, *Container Handbook* 2003

Chapter 2

Implementation of An Active RFID System

2.1 RFID System hardware design and related protocol

There are two major RFID standard bodies, namely, EPCglobal and ISO. For different applications people adopt different standards. Only the products which have the same standard can communicate with each other.

The EPCglobal organization has four different specifications for passive RFID systems—900MHz Class 0 RFID Tag Specification, 13.56 MHz ISM Band Class 1 RFID Tag interface Specification, 860MHz—930MHz Class 1 RFID Tag Radio Frequency & Logical Communication Interface Specification and Class-1 Generation-2 UHF RFID Conformance Requirements Specification v.1.0.2. Three of them are for UHF RFID systems and one is for HF RFID system. All of these specifications are for passive RFID systems. The 13.56 MHz ISM Band Class 1 specification is for very short distance applications such as small item management. The distance between tags and readers will not exceed 1 meter due to strong magnetic coupling method. The other three specifications—Class 0, Class1 and Class1Generation2 are electromagnetic coupling so that the distance between tags

and readers is longer than the 13.56 MHz Class 1 specification. In some cases the communication distance can reach 10 meters.

Compared with EPCglobal standards, ISO 18000 also has a series of RFID standards. There are seven sub standards according to different operating frequency. ISO 18000-1 includes reference architecture and definition of parameters to be standardized. ISO 18000-2 includes parameters for air interface communications below 135 kHz. Standards from ISO 18000-3 to ISO 18000-6 include parameters for air interface communications at 13.56 MHz, 2.45 GHz and 860 MHz to 960 MHz, respectively. ISO 18000-7 includes parameters for active air interface communications at 433 MHz. ISO 18000-7 is the only standard for active RFID system among all RFID standards and the main applications of ISO 18000-7 are focused on distance greater than 10 meter. One can see that ISO 18000-7 is the only choice for an active RFID system.

A full Active RFID system includes tags, readers and reader controllers. A tag can be separated into 2 main parts. First of all, it needs a transceiver to receive or transmit signal between itself and readers. Secondly, it needs a base band controller to control all the data format and different states according to ISO 18000-7. And the base band controller also needs enough memory size to store all the information which will be carried by tags. Power saving is a major issue for active tags because there is only a small battery on every small tag. A typical battery capacity is

1000mAh. A tag should last several years by using this small battery. Thus the transceiver and the base band controller should be very low power consumption devices. Here we choose CC1000 IC chip, which is developed by Chipcon, as tags' transceiver and MSP430, which is developed by TI, as tags' base band controller. Both of these two devices are very low power consumption. Figure2.1.1 is the hardware block diagram for a tag.

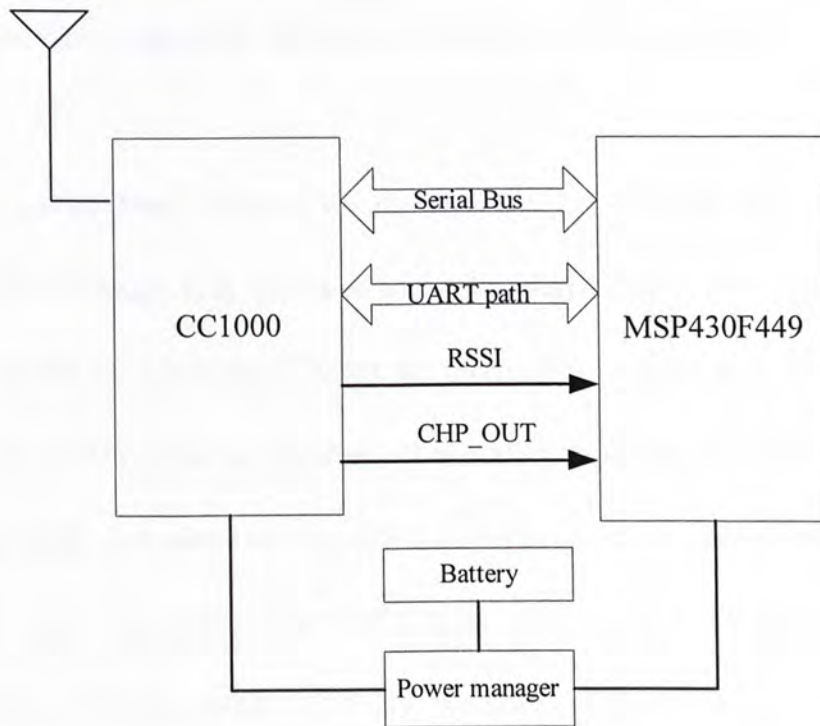


Figure 2.1.1 Hardware Structure of Tag

From this diagram we note that a tag is consist of five parts—antenna, CC1000, MSP430F449, Battery and Power management IC(SP6201). SP6201 is a DC to DC module which provides a stable 3.3V power supply and maximum 200 mA output current for other circuits. It is also an ultra low power consumption IC. The maximum shutdown current is $1\mu A$ and the ground current is $28\mu A$ when the load current is $100\mu A$ [1]. This power management IC also provides ultra accurate

DC output voltage which can be as accurate as 2% of the output voltage.

The battery's rated capacitor is 1650mAh and the rated voltage is 3.6 V. The leakage current of this battery is very low [2]. It has been proved that this battery can be stored for 10 years under a normal room temperature. For our design aim, a tag should last at least 3 years. Thus the leakage current of the battery should be as small as possible. Apparently this kind of battery fits our requirements.

From the system block diagram we also note that the CC1000 is connected with MSP430F449 through four groups of wires. The Serial Bus is used to configure all registers which are inside the CC1000. The Serial Bus includes three lines—PCLK, PDATA and PALE. After configuring all necessary registers, CC1000 will start to operate properly and automatically. All these registers do not need to be configured during the operating period. The UART signal path is used to receive and transmit data between CC1000 and MSP430F449. It consists of two lines—DIO and DCLK. These two lines have different functions due to different operating mode. In Synchronous NRZ mode and Synchronous Manchester encoded mode, DCLK provides synchronous clock to MCU and DIO is used to transfer data. However, in Transparent Asynchronous UART mode, DCLK is not used in transmit mode but it is used as a data output pin in receive mode. On the contrary, DIO is not used in receive mode but it is used as a data input pin in transmit mode. RSSI is used to indicate the signal strength which is received by CC1000. The RSSI signal is a very

important signal in our wake-up strategy. The last path is the CHP_OUT. This path can be used as PLL Lock indicator. It is useful for frequency hopping applications.

Compared with tags, readers must have the capability to communicate with computers. Thus we need to add some communication ICs into readers' hardware design. Obviously a reader does not have power saving problems and power supply is provided by outside device so that it does not need a battery. The hardware block diagram of a reader is shown as below:

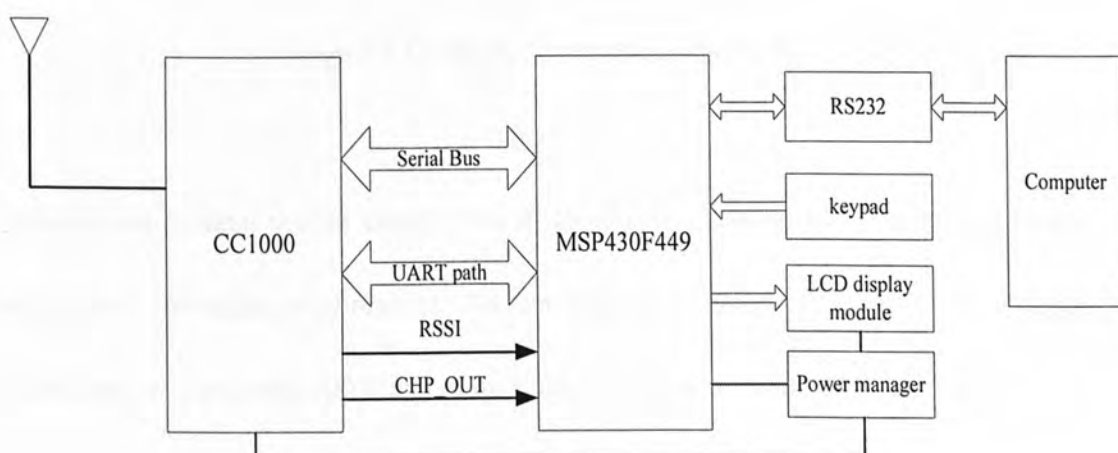


Figure 2.1.2 Hardware Structure of a Reader

From this diagram we note that the communication between a reader and a computer is through RS232 port. The keypad and LCD display module are all optional modules. This hardware structure of a reader is a fundamental structure. Base on this structure we can still add lots of functions such as memory size extension, WLAN or TCP/IP modules.

The full system including tags, readers and reader controllers is shown in Figure

2.1.3.

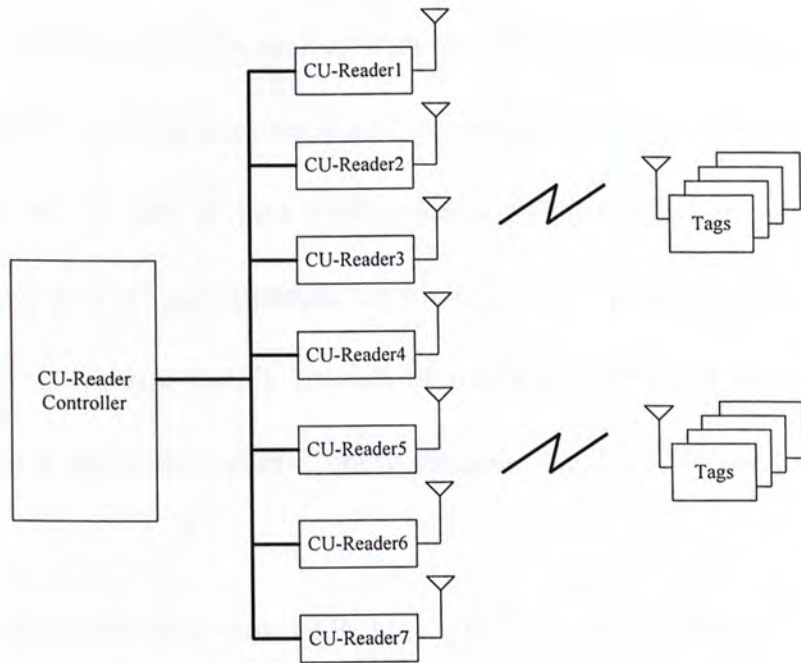


Figure 2.1.3 Whole System Block Diagram

In the system, each reader controller can handle seven readers. This is due to the large area coverage requirement. As we already mention in chapter 1, a large container yard is about 100,000 square meters. A single reader can not cover such a large region so that we need large amounts of readers to operate relatively. Every seven readers will form a group and connect to a reader controller through wire connection such as RS232 or wireless connection such as WLAN. All reader controllers will connect together through intranet. The main task of reader controllers is to collect all the useful data which is received by readers and transmit them to a middleware or send the data which is from middleware to particular readers.

2.2 Introduction to ISO 18000-7 [3]

Our active RFID system is compliant with ISO 18000-7. Some of the key features of ISO 18000-7 must be introduced first. As we mention in previous chapter, ISO 18000-7 is the 7th part of ISO 18000—Radio frequency identification for item management. This 7th part is parameters for active air interface communications at 433MHz. The standard mainly consists of four parts—Physical layer, Data Link layer, Physical and Media Access Control parameters and Anti-collision parameters.

Firstly, the active RFID system is a Reader-Talk-First system. Physical layer defines the RF communication link between interrogator and tag utilizes narrow band UHF frequency with the following characteristics:

Carrier Frequency	433.92 MHz \pm 20 ppm
Modulation Type	FSK
Frequency deviation	\pm 50 kHz
Symbol Low	$f_c + 50$ kHz
Symbol High	$f_c - 50$ kHz
Modulation rate	27.7 kHz
Wake up Signal	30 kHz

The Wake up Signal is a special signal in this communication system. Actually it is the biggest difference when compared with a general communication system. The Wake Up signal is transmitted by interrogator for minimum of 2.5 seconds to wake up all tags with communication range. A wake up signal is a 30 kHz sub-carrier

tone.

Data Link Layer defines data format between tags and readers. Data is transmitted in packet format. A packet is comprised of a preamble, data bytes and a final logic low period. A full data packet is shown in Figure 2.2.1

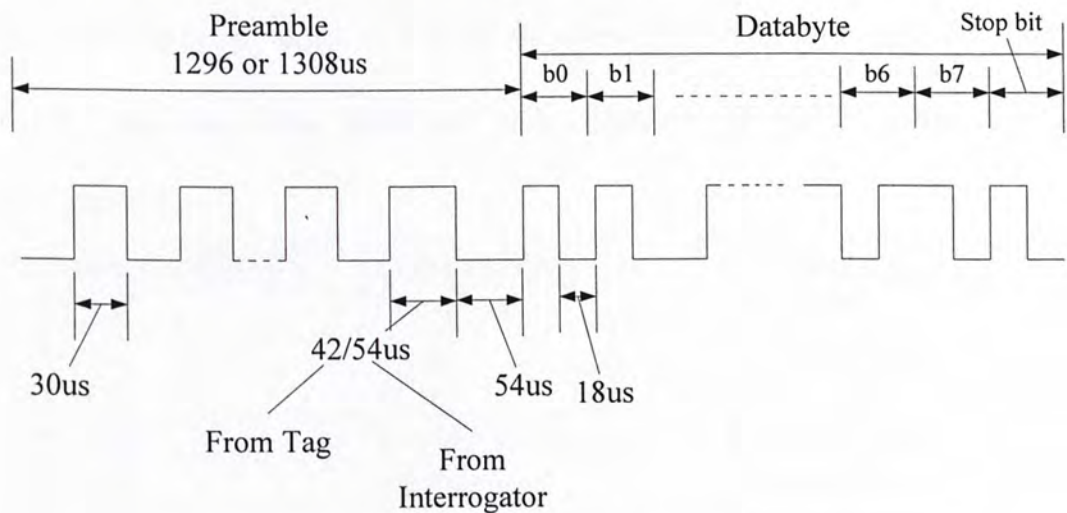


Figure 2.2.1 Data Packet Format

A preamble is comprised of twenty pulses of $60\mu s$ period, $30\mu s$ high and $30\mu s$ low, followed by a final sync pulse which identifies the communication direction: $42\mu s$ high $54\mu s$ low(Tag to Reader); $54\mu s$ high $54\mu s$ low(Reader to Tag); Data bytes are in Manchester code format, comprised of 8 bits and one stop bit. Every bit period is $36\mu s$. The stop bit is coded as a zero bit. In this protocol a CRC checksum is calculated as a 16-bit value according to CCITT polynomial $(x^{16} + x^{12} + x^5 + 1)$. A final period of $36\mu s$ continuous logic low is transmitted in each packet after the CRC bytes.

Message format form reader to tag is shown in Table 2.2.1

Command Prefix	Command Type	Owner ID	Tag ID	Interrogator ID	Command Code	Parameters	CRC
1 byte ('31')	1 byte (8 bits)	3 bytes	4 bytes	2 bytes	1 byte	N bytes	2 bytes

Table 2.2.1 Reader to Tag Message Format

Command code takes 1 byte in the whole message. There are two kinds of Command code. One is for broadcast from reader to tag another is for point to point communication. In Table 2.2.2 there are some frequently used command codes. Using these command codes the basic functions of RFID system can be implemented.

Command code(R/W)	Command name	Command type
'10'/NA	Collection	Broadcast
NA/ '15'	Sleep	Point to Point
'01'/NA	Status	Point to Point
'60'/'E0'	Read/Write Memory	Point to Point
NA/ '95'	Set Password	Point to Point
'17' / '97'	Set password protect	Point to Point

Table 2.2.2 Command codes

Tag to reader message has two different formats—Broadcast response message format and Point-to-Point response message format. They are shown in Table 2.2.3 and Table 4, respectively.

Tag Status	Message Length	Int ID	Tag ID	Owner ID	User ID	Data	CRC
2 bytes	1 byte	2 bytes	4 bytes	3 bytes	0~16 bytes	0~N bytes	2 bytes

Table 2.2.3 Broadcast response message format

Tag Status	Message Length	Int ID	Tag ID	Command Code	Parameters	CRC
2 bytes	1 byte	2 bytes	4 bytes	1 bytes	N bytes	2 bytes

Table 2.2.4 Point-to-Point response message format

Every RFID system will face the multi tag problem and there are different kinds of solutions for it. For instance, Binary search algorithm and ALOHA procedure are all popular anti-collision algorithm. This standard also proposes its algorithm. It is similar to ALOHA procedure. The whole anti-collision procedure is shown in Figure 2.2.2.

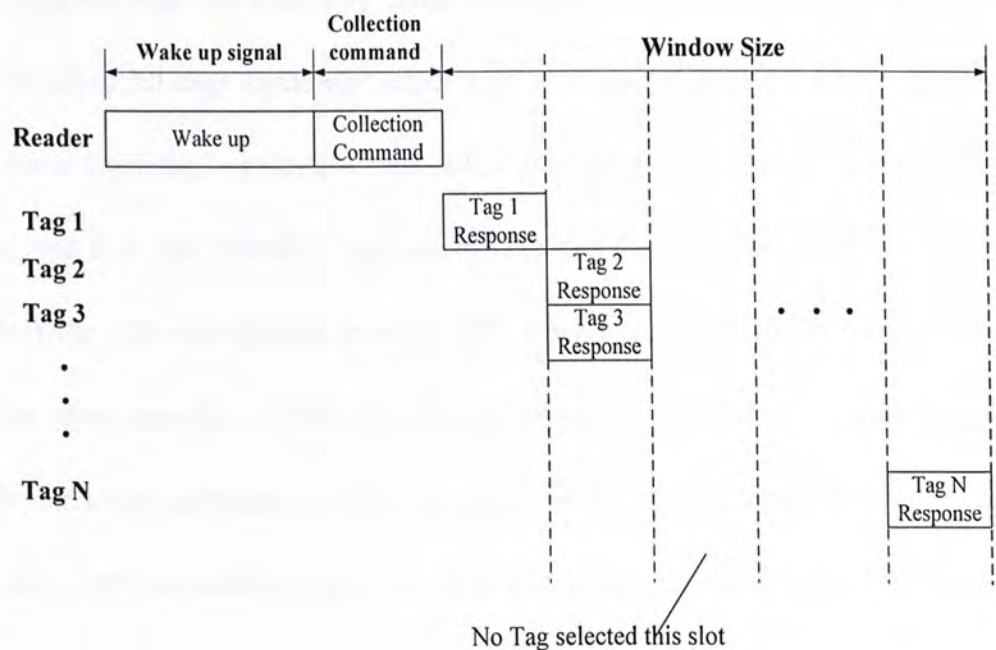


Figure 2.2.2 Anti-collision between multiple tags and single reader

From this figure we can clearly know the whole procedure of anti-collision between multiple tags and single reader. First of all, the communication between reader and tag is Master-Slave mode. Thus Reader will firstly send out a wake up signal. As we describe in the previous session, a wake up signal is a 30 kHz sub-carrier and it will

last at least 2.5 seconds. A collection command will follow the wake up signal and broadcast to tags. After broadcasting the collection command the reader will turn to receive mode and try to receive all possible responses from tags. Tags work in slave mode during the whole process of anti-collision and all their reactions are according to reader's command. First of all, tags are all in sleep mode for saving power and they will try to capture a wake up signal periodically. When tags capture the wake up signal they will be awake and turn to receive mode. Tags will wait for a collection command which is send by a reader in the receive mode. After tags capture the collection command tags and the reader are synchronous. After synchronization tags will randomly select a time slot to transfer their Tag ID to the reader. Because all tags randomly select time slots to transmit their ID, collision occurs when two tags or several tags select the same time slot to transmit. For instance, we find that collision happens in time slot 2(see Figure 2.2.2). A reader can detect the collision through invalid CRC. Then reader will try to receive valid tag ID in other time slots. When the collection round is completed the reader starts transmitting sleep command to the tags which is already collected by the reader during the previous collection ground. Tags that receiving sleep command turn to sleep mode and do not participate in collection in the subsequent collection rounds.

The reader will send collection command again in the next round and only tags which do not receive the sleep command will response to it and randomly select time slots to transmit their tag IDs. The collision probability is much lower than the

previous round in this round. Eventually during several rounds all tags IDs will be collect by reader and this process will continue until no more tags are being detected during three subsequent collection rounds. This kind of anti-collision method is defined as Slot- ALOHA.

2.3 Microcontroller specification [4]

Firstly, the data rate of this active RFID system is 27.7kbit and Data bytes are in Manchester code format. Thus the data rate is doubled to 55.4kbit and we need a fast MCU to decode the data. Secondly, every data packet has a preamble which has $30\mu s$ pulse and $54\mu s$ pulse. MCU should fast enough to detect this $14\mu s$ difference between them otherwise tags or readers can not distinguish the beginning of data from the whole data packet. There are two ways to increase the speed of MCU—increasing the system clock of MCU or increasing the bits of MCU. Increasing the system clock of MCU will also increase power consumption. Thus we choose 16-bit MCU instead of 8-bit MCU. The 16-bit MCU is much faster than 8-bit MCU. Thirdly, the memory size of MCU should be at least 60kbyte according to our design aim. Fourthly, the MCU should also have plenty of peripherals such as ADC and Timer for data decoding. Finally the MCU must be an ultra low power consumption device.

Due to the above requirements finally we choose MSP430F449 as our base band

microcontroller. The TI MSP430 family is an ultra low power microcontroller which consists of different sets of peripherals. It has five low power modes for different applications and especially for portable battery support devices. This MCU includes a powerful 16-RSIS CPU, 16-bit registers and constant generators that attribute to maximum code efficiency. Some of the key features of MSP430F449 are shown below:

- Ultra low-Power Consumption:
 - Active Mode: $280\mu A$ at 1 MHz, 2.2 V
 - Standby Mode: $1.1\mu A$
 - Off Mode (RAM Retention): $0.1\mu A$
- Five Power Saving Modes
- Wake up From Standby Mode in $6\mu s$
- 12-Bit A/D Converter With Internal
- Reference, Sample-and-Hold and Auto Scan Feature
- 16-Bit Timer_A With Three Capture/Compare Registers
- Serial Communication Interface (USART)
- Serial Onboard Programming, No External Programming Voltage Needed
- Programmable Code Protection by Security Fuse
- 60KB+256B Flash Memory, 2KB RAM
- FLL+ Clock Module

Several key features must be mentioned here. First of all, the MCU has five power saving modes. We use two power saving modes in our design. One is active mode

(AM) another is Low power mode3 (LPM3). In LPM3 mode, the power consumption is $0.9\mu A$. In active mode, the power consumption is about $280\mu A$ at 1 MHz. Secondly, the receive signal strength indicator from CC1000 is between 0V and 1.2V. An ADC is used to convert this analog signal to digital signal. There is a 12-Bit A/D inside this MCU. The maximum conversion of this ADC is 200ksps and the conversion can be initiated by software or hardware such as Timer. Another very useful function for power saving is that the ADC core and reference voltage can be power down separately. This is important for power saving because ADC also consumes $1mA$ during sampling and conversion period. Other details will be given in the section of programming.

2.4 RF Model Specifications

The hardware part of a tag is separated into two parts—base band module and RF module. The base band module is MSP430F449 and the RF module is CC1000 which is a very low current consumption UHF RF transceiver. This IC can be programmed via a serial bus. Some key features of CC1000 which are important for our design are listed here:

- Very low current consumption
 - Receive mode: $7.4mA$ at 433MHz
 - Transmit mode: $14.8mA$ at 433MHz and output power is 5dBm
 - Power Down mode: $0.2\mu A$

- Frequency range 300-1000 MHz
- Integrated bit synchronizer
- RSSI output
- FSK data rate up to 76.8kBaund
- Programmable frequency in 250 Hz steps

Form all these features we know that CC1000 can be adopt as the RF section for tags which are compliant with ISO 18000-7. The RSSI is important in our Active RFID system. We used the RSSI as a threshold to control the communication distance between tags and reader. Actually, this RSSI is an analogue output signal at the RSSI pin and the output current of this pin is inversely proportional to the input signal level. The RSSI voltage rage from 0~1.2V and the indicated input signal level is from -50dBm to -105dBm. A high voltage indicates a lower input signal. Due to a RSSI voltage vs. input power curve the input power can be calculated using the following equations:

$$P_{in} = -51.3 * V_{RSSI} - 49.2 \quad (dBm) \quad \text{At 433MHz} \quad (2.4.1)$$

After setting the input signal threshold only the input signal which is larger enough can wake up a tag.

2.5 Communication Between A PC and A Reader

Communications between PC and Reader is via RS232 port. The communication distance is about 50 feet. RS232 communication is easy to develop. It does not need

a driver between computer and a reader. There are only three wires between them—TXD, RXD and GND. The MCU also provide USART interference between it and the computer. The USART supports synchronous SPI (3 or 4 pin) and asynchronous UART communication protocols, using double-buffered transmit and receive channel. However, the output voltage of MCU is 0V and 3.3V and the voltage level of RS232 is +5V~+15V (positive level) and -5V~-15V (negative level). Thus we need a conversion IC between a MCU and RS232 of a computer. Here we choice MAX3221E, a RS232 transceiver, as the conversion IC. Some of its features are shown below:

- 1 μ A Supply Current Achieved with AutoShutdown
- Small 0.1 μ F Capacitors
- Guaranteed 120kbps Data Rate
- True RS-232 Operation from VCC = +3.0V to +5.5V
- Smallest Single-Supply RS-232 Transceiver

2.6 Programming

All the programs are base on the hardware. The main task of the software part is to make tags and readers work properly and save power as much as possible. Usually power saving will include two parts. Obviously the first part is hardware part. The hardware should has the capability to work in a standby mode for saving power and active mode for transmit and receive mode. The second part is working sequences

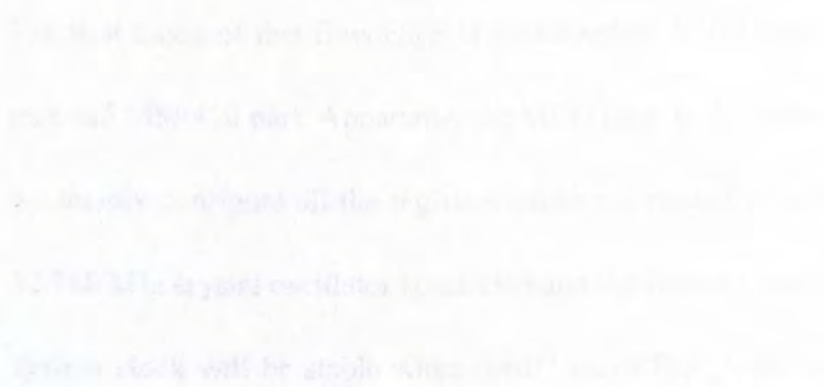
of tags which are controlled by software. The working sequence is according to different applications. A principle of the working sequence is to ensure tags only active during transmitting or receiving data. Tags should maintain power down mode or standby mode during other times.

The whole program is separated into several main parts—Data reception, Data transmission, Manchester coding and decoding, Anti-collision and CRC checksum. Much more details will be given in the following sections.

2.6.1 Procedure sequences of Reader and Tag

An active RFID system is a reader-talk-first system or a master-slaver system. Thus all the actions of tags are controlled by a reader. The flow chart of a reader is shown in Figure 2.6.1.1:

Figure 2.6.1.1: Reader procedure sequence



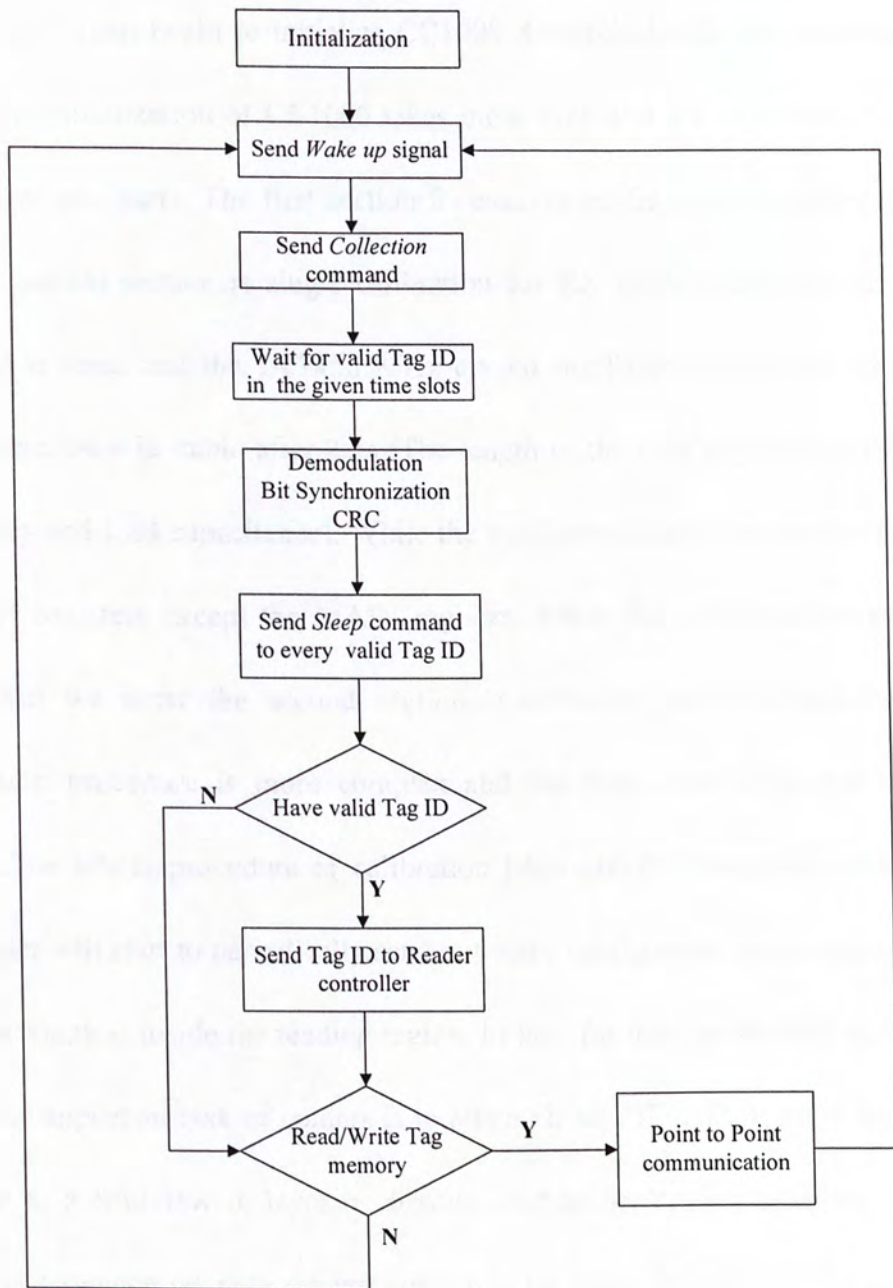


Figure 2.6.1.1 working sequence of Reader

The first block of this flow chart is initialization. Initialization consists of CC1000 part and MSP430 part. Apparently the MCU must be initialized firstly. At this stage we mainly configure all the registers which are related to system clock of MCU. A 32.768 kHz crystal oscillator is selected and the system clock is set to 3.3 MHz. The system clock will be stable when the 0th bit of FLL_CTL0 registers turns to zero.

After that we can begin to initialize CC1000. Compared with the initialization of MCU, the initialization of CC1000 takes more time and it's more complicated. It consists of two parts. The first section focuses on configuring all related registers and the second section is single calibration for RX mode and TX mode. Firstly CC1000 is reset and the 14.7456 MHz crystal oscillator will be turned on. The crystal oscillator is stable after 2ms (The length of the time depends on the crystal frequency and load capacitance). While the oscillator is stable we start to configure all other registers except the MAIN register. When this configuration process is completed we enter the second section—Calibration of VCO and PLL. This calibration procedure is more complex and the flow chart is shown in Figure 2.6.1.2. The whole procedure of calibration takes about 350ms. After initialization the reader will start to periodically send out wake up signal and try to capture all the tag IDs which is inside the reading region. In fact, for the contain yard management the most important task of readers is to attain all tags IDs. Then these tag IDs will be sent to a Middleware layer or directly send to application software. From the working sequence we note the left column is for collecting tag ID. The right lower block is for Point-to-Point data transmission. The detail of Point-to-Point communication flow chart is shown in Figure 2.6.1.3.

At Point-to-Point communication stage, firstly a reader will send out a wake up signal and all tags which are within this region will be aware and wait for the command. Then the reader will broadcast a read or write command with tag ID.

Only a tag with the same tag ID will respond the commands enter the Point-to-Point communication stage. Usually the data is less than 1kbyte. If the size of data is more than 1kbytes, the data will split into several sections. Every section is 1kbytes. After receiving all the sections the reader or tag will combine them to a complete data packet. Now the data rate is 27.7kbits/second. Thus transmitting 1kbytes needs 326ms. To make sure every time tags or readers do not miss the preamble of the data when receiving data, every receiving section needs to wait 350ms+16ms.

To ensure receiving data correctly, tags or readers will wait for a reply after sending out data. If the reply is incorrect, data will be transmitted again. However, every unit section of data will not be resent more than 3 times. If one section of the whole data is transmitted more than 3 times, the communication will be marked as failed.

We only show the flow chart of Point-to-Point communication of Reader. Actually the Point-to-Point communication procedure of tag is almost the same as Reader. The only difference is that a tag will not send out wake up signal instead of trying to capture a wake up signal. After a tag captures a wake up signal and attains a read or write data command, it will turn to sending or receiving data process.

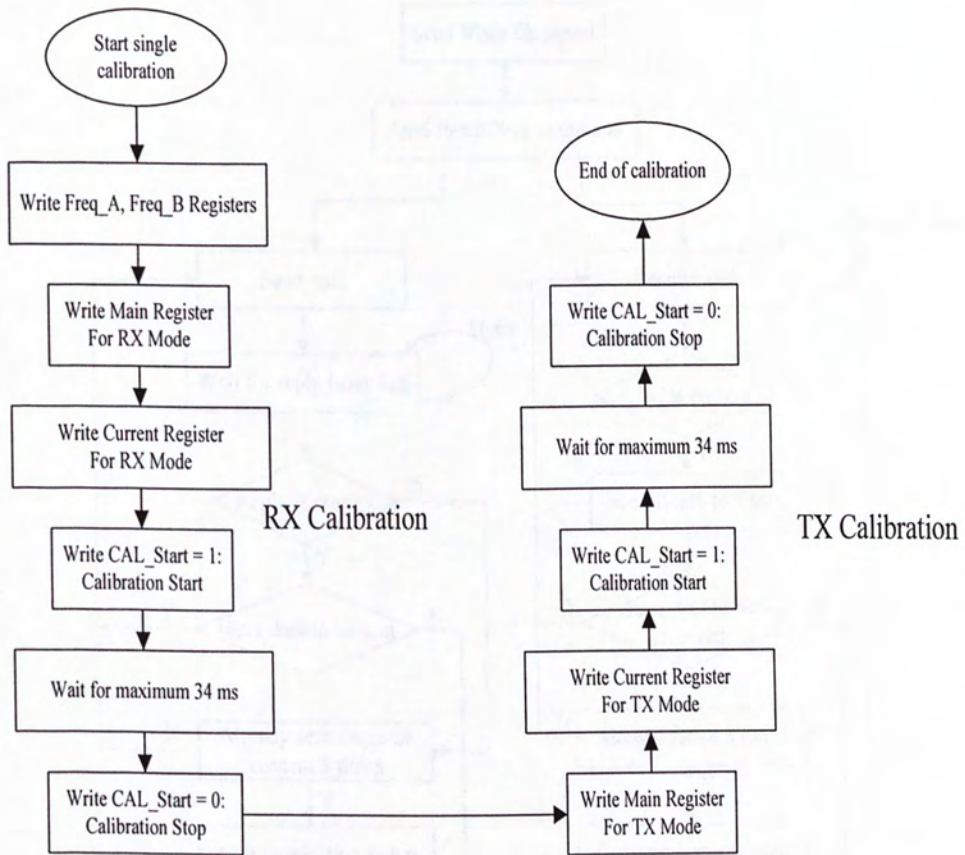


Figure 2.6.1.2 Calibration for RX and TX mode

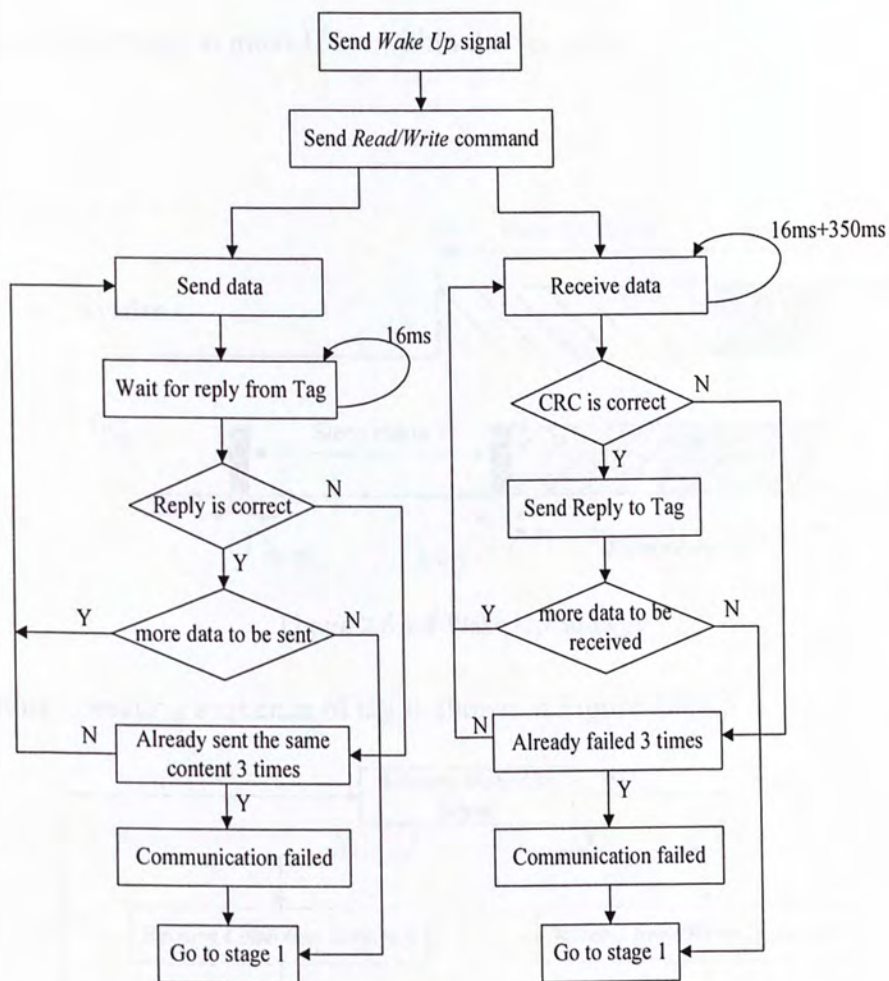


Figure 2.6.1.3 Point-to-Point Communication procedure of Reader

Compared with the whole communication procedure of readers, the procedure of tags has some differences. One important character of a tag is that every tag's energy is from a small battery. Thus one major aim of tags is to save power. Due to this reason most of time tags maintain in the sleep mode. They will be awaked up periodically. This procedure is shown in Figure 2.6.1.3. We call the action that a tag is awake for capturing the wake up signal as sniff. We note that a sniff time is very short when compared with a sleep time. Usually the sniff time is less than 10ms. In one period a sniff action plus sleep time is 2.5 seconds. This means a tag will

maintain active mode at most 10ms within 2.5 seconds.

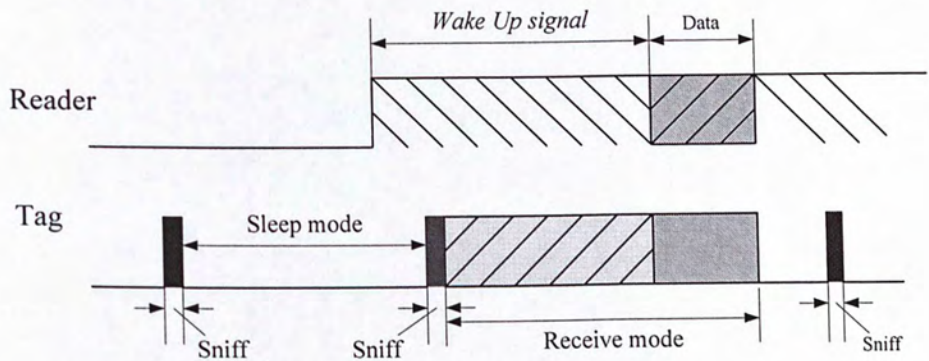


Figure 2.6.1.4 Wake Up Strategy

The whole operating sequence of tag is shown in Figure 2.6.1.5

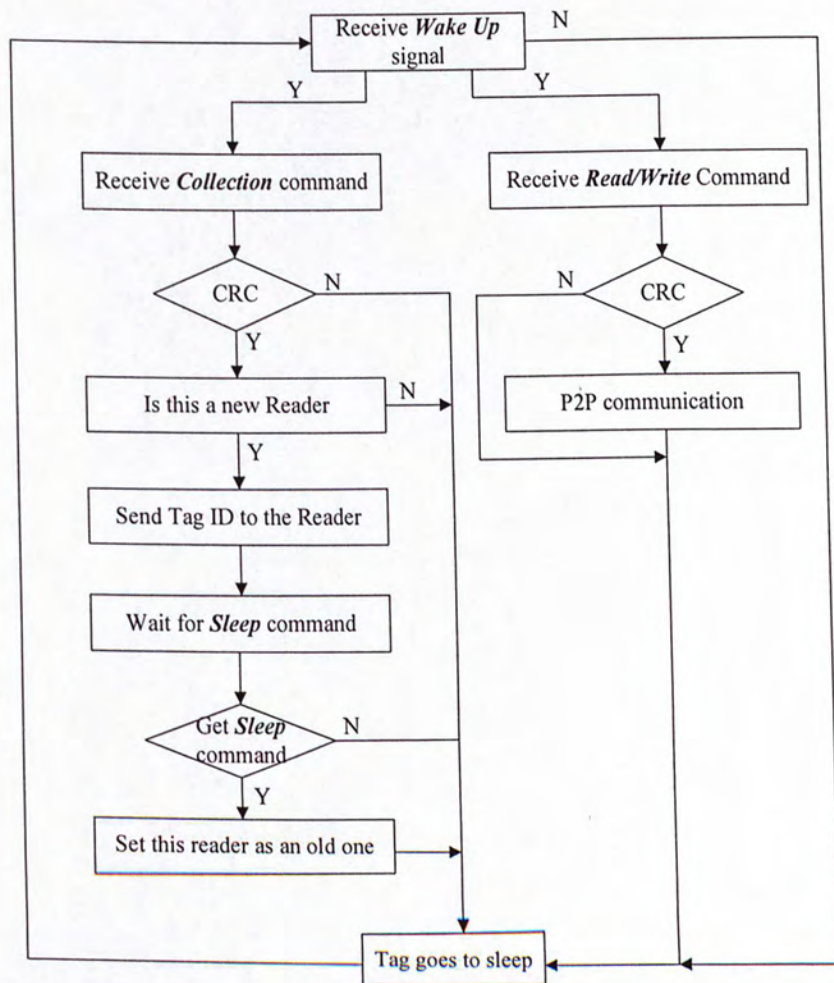


Figure 2.6.1.5 Operating Sequence of Tag

In figure 2.6.1.5 we find that a tag will judge whether the collection command is sent by a new reader or not. This is also according to the power saving principle. Our application is contain yard management. It means tags will stay in the same place for a long time. A tag will capture lots of collection command during this long time. If every time the tag replies to this collection command, it will waste too much power. Thus tags only need to report their ID to a new reader and after that tags should ignore all other collection commands which are sent by this reader.

2.6.2 Sequence of data transmission and reception

According to ISO 18000-7 all data are transmitted in packet format. The packet format is shown in figure 2.6.2.1.

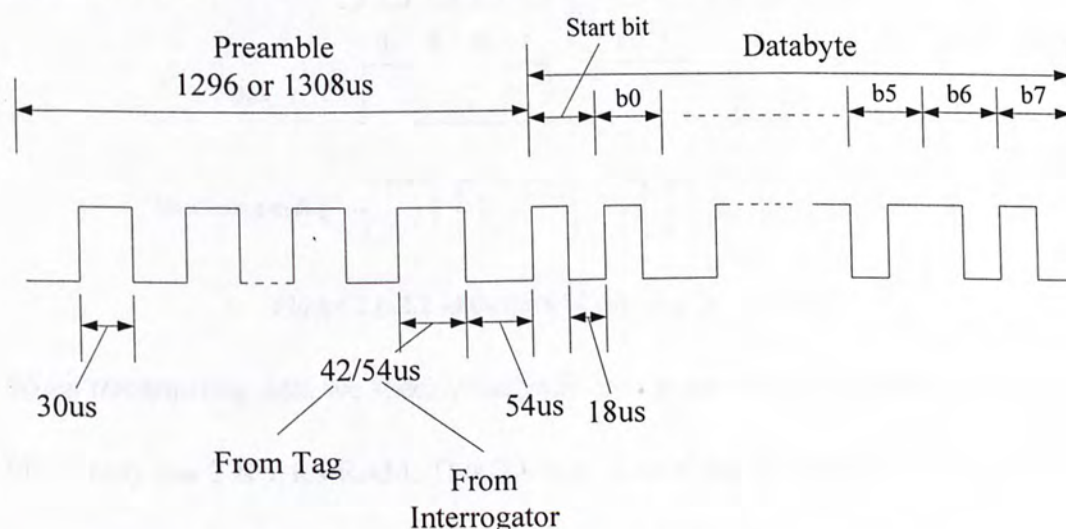


Figure 2.6.2.1 Data Packet Format

Every data packet starts with a preamble. A preamble consists of twenty pulses of 60 μs period, 30 μs high and 30 μs low, followed by a final sync pulse which

identifies the communication direction. All valid data which follow the preamble are transmitted in Manchester format. Manchester encoding is also called Split-Phase coding. Logic '1' is represented by a negative edge. Logic '0' is represented by a positive edge. It can also be viewed as logic '1' is encoded by a negative 90 degree phase transition and logic '0' is encoded by a positive 90 degree phase transition. This transition is happened in the middle of each bit period. This is the reason that Manchester encoding is also called Split-Phase coding. Because data in Manchester format will not have a long period '0' or '1', it is easy to recover data clock form data. The waveform of a Manchester encoding data stream is shown in figure 2.6.2.2.

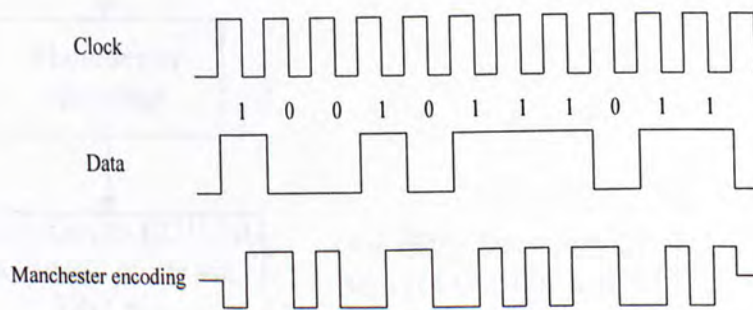


Figure 2.6.2.2 Manchester Encoding Data Stream

When transmitting data we specify the valid data must at most 1Kbytes because the MCU only has 2 Kbytes RAM. This 2 Kbyte is working as a data buffer. If the data is larger than 1 Kbytes, it will be separated into several packets and every data packet is less than 1Kbytes. A flow chart of transmitting one packet is shown in Figure 2.6.2.3. The buffer size includes three parts. The first part is for the valid data. The second part is for start bits and the last part is for CRC checksum.

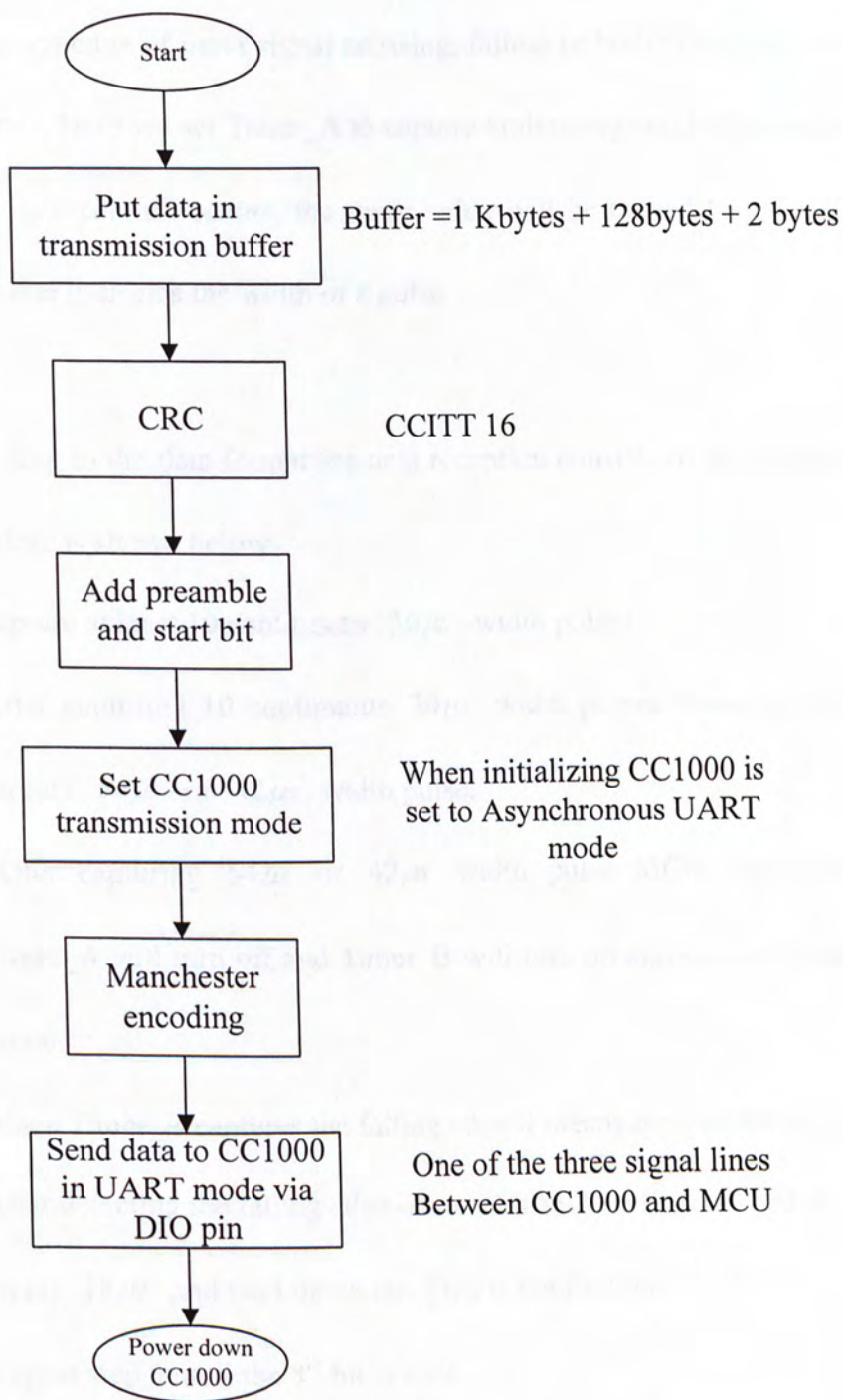


Figure 2.6.2.3 Data Transmission

Compared with data transmission, data reception is more complicated. To detect the pulse width we need to use Timer_A which is a build-in timer of MSP430F449. Timer_A has capture/compare blocks. When Timer_A is in capture mode it can

capture the edge of input signal as rising, falling or both according to the setting of CMx bits. Here we set Timer_A to capture both rising and falling edges of an input signal. If a capture occurs, the timer value will be copied to a TACCRx register. This value indicates the width of a pulse.

According to the data format the data reception consists of ten sections. The whole procedure is shown below:

- (1) Capture at least 10 continuous $30\mu s$ width pulses.
- (2) After capturing 10 continuous $30\mu s$ width pulses Timer_A will be ready to capture $54\mu s$ or $42\mu s$ width pulse.
- (3) After capturing $54\mu s$ or $42\mu s$ width pulse MCU will delay $56\mu s$ and Timer_A will turn off and Timer_B will turn on and set to capture falling edge mode.
- (4) When Timer_B captures the falling edge it means the start bit is detected.
- (5) After detecting the falling edge of start bit MCU will delay $27\mu s$
- (6) Delay $18\mu s$ and read the value. This is the first bit.
- (7) Repeat step 6 until the 8th bit is read.
- (8) Delay $18\mu s$ and Time_B will try to capture a start bit of next byte.
- (9) When the start bit is captured, step 6 and step 7 will be repeated until the 8 bits are read.
- (10) The procedure will stop until the end byte is detected.

From the above procedure we note that step 6 and step 7 is Manchester decoding. We also note that there is a start bit for every eight bits. After decoding eight bits data Timer_B will wait for an edge of a start bit. This means there is a data synchronization bit for every eight bits.

2.6.3 CRC implementation

CRC is easier to encode and decode than lots of linear block. The encoding operation is easily performed using shift register or software. Further more, implementation of the decoder becomes more practical due to its simple algebraic structure [6]. There are lots of methods to implement CRC. CRC is base on linearity encoding theory. A CRC checksum will be generated according to a generator polynomial and data which needs to be encoded. This generated checksum is attached to the end of data and transmitted to receiver.

To generate a checksum, data will be left shifted 16 bits (for a 16-bit CRC) and divided by a specified generator polynomial. The division yields a quotient and a remainder. The remainder is the checksum. This relationship is shown in the following expression [7]:

$$\frac{B(x) \cdot 2^{16}}{G(x)} = Q(x) + \frac{R(x)}{G(x)} \quad (2.6.3.1)$$

$B(x)$: N bits binary data sequence.

$G(x)$: Generator polynomial

$Q(x)$: Quotient

$R(x)$: Remainder

First of all, a binary sequence can express as:

$$B(x) = B_n \cdot 2^n + B_{n-1} \cdot 2^{n-1} + \dots + B_1 \cdot 2 + B_0 \quad (2.6.3.2)$$

To calculate the checksum of $B(x)$ firstly $B(x)$ will be left shift 16 bits and then divided by a generator polynomial. In ISO 18000-7 it already specifies the generator polynomial is $(x^{16} + x^{12} + x^5 + 1)$.

$$\frac{B(x) \cdot 2^{16}}{G(x)} = \frac{B_n \cdot 2^{16}}{G(x)} \cdot 2^n + \frac{B_{n-1} \cdot 2^{16}}{G(x)} \cdot 2^{n-1} + \dots + \frac{B_1 \cdot 2^{16}}{G(x)} \cdot 2 + \frac{B_0 \cdot 2^{16}}{G(x)} \quad (2.6.3.3)$$

$$\text{Set: } \frac{B_n \cdot 2^{16}}{G(x)} = Q_n(x) + \frac{R_n(x)}{G(x)} \quad (2.6.3.4)$$

Then substitute expression (2.6.3.4) into (2.6.3.3):

$$\frac{B_n \cdot 2^{16}}{G(x)} = Q_n(x) \cdot 2^n + \left\{ \frac{R_n(x) \cdot 2}{G(x)} + \frac{B_{n-1} \cdot 2^{16}}{G(x)} \right\} \cdot 2^{n-1} + \dots + \frac{B_1 \cdot 2^{16}}{G(x)} \cdot 2 + \frac{B_0 \cdot 2^{16}}{G(x)} \quad (2.6.3.5)$$

$$\text{Set: } \frac{R_n(x) \cdot 2}{G(x)} + \frac{B_{n-1} \cdot 2^{16}}{G(x)} = Q_{n-1}(x) + \frac{R_{n-1}(x)}{G(x)} \quad (2.6.3.6)$$

Substitute expression (6) into (5) and follow the same procedure finally we get:

$$\frac{B_n \cdot 2^{16}}{G(x)} = Q_n(x) \cdot 2^n + Q_{n-1}(x) \cdot 2^{n-1} + \dots + Q_0(x) + \frac{R_0(x)}{G(x)} \quad (2.6.3.7)$$

$R_0(x)$ is the final remainder of the binary stream.

From the above analysis, especially expression (2.6.3.6), we note that the CRC code of this bit can be attained according to the remainder of last bit. And follow this procedure the final CRC code can be calculated. However, this procedure is slow

because a CRC remainder can only be calculated bit by bit. It takes lots of times. To increase the calculation speed we usually calculate CRC remainder according to byte instead of bit [7]. Firstly, a binary data stream can be express as:

$$B(x) = B_n \cdot 2^{8n} + B_{n-1} \cdot 2^{8(n-1)} + \dots + B_1 \cdot 2^8 + B_0 \quad (2.3.6.8)$$

And the CRC code of $B(x)$ is calculated by:

$$\frac{B(x) \cdot 2^{16}}{G(x)} = \frac{B_n \cdot 2^{16}}{G(x)} \cdot 2^{8n} + \frac{B_{n-1} \cdot 2^{16}}{G(x)} \cdot 2^{8(n-1)} + \dots + \frac{B_1 \cdot 2^{16}}{G(x)} \cdot 2^8 + \frac{B_0 \cdot 2^{16}}{G(x)} \quad (2.3.6.9)$$

Then substitute (2.6.3.4) into (2.3.6.9) and we get

$$\frac{B_n \cdot 2^{16}}{G(x)} = Q_n(x) \cdot 2^{8n} + \left\{ \frac{R_n(x) \cdot 2^8}{G(x)} + \frac{B_{n-1} \cdot 2^{16}}{G(x)} \right\} \cdot 2^{8(n-1)} + \dots + \frac{B_0 \cdot 2^{16}}{G(x)} \quad (2.3.6.10)$$

Because:

$$\begin{aligned} R_n(x) \cdot 2^8 &= [R_{nH8}(x) \cdot 2^8 + R_{nL8}(x)] \cdot 2^8 \\ &= R_{nH8}(x) \cdot 2^{16} + R_{nL8}(x) \cdot 2^8 \end{aligned}$$

Thus (2.3.6.10) can be changed to

$$\begin{aligned} \frac{B_n \cdot 2^{16}}{G(x)} &= Q_n(x) \cdot 2^{8n} + \left\{ \frac{R_{nL8}(x) \cdot 2^8}{G(x)} + \frac{[R_{nH8}(x) + B_{n-1}(x)] \cdot 2^{16}}{G(x)} \right\} \cdot 2^{8(n-1)} \\ &\quad + \dots + \frac{B_0 \cdot 2^{16}}{G(x)} \end{aligned} \quad (2.3.6.11)$$

Set:

$$\frac{R_{nL8}(x) \cdot 2^8}{G(x)} + \frac{[R_{nH8}(x) + B_{n-1}(x)] \cdot 2^{16}}{G(x)} = Q_{n-1}(x) + \frac{R_{n-1}(x)}{G(x)} \quad (2.3.6.12)$$

Finally we get:

$$\frac{B_n \cdot 2^{16}}{G(x)} = Q_n(x) \cdot 2^{8n} + Q_{n-1}(x) \cdot 2^{8(n-1)} + \dots + Q_0(x) + \frac{R_0(x)}{G(x)} \quad (2.3.6.13)$$

$R_0(x)$ is the final remainder.

From expression (2.3.6.12) we note that a CRC of current byte is according to the CRC of last byte. All the CRC value is calculated byte by byte instead of bit by bit.

We can also make a table for all the possible CRC value of 8 bits binary data. Each time when calculating a CRC value we only need to find out the value from the table and no calculation is needed. The speed will be improved a lot. The table according to CCITT polynomial $(x^{16} + x^{12} + x^5 + 1)$ is shown in appendix.

2.7 Testing result

The communication distance between tags and readers is tested in this section. Current consumption is also tested according to different operating mode. A tag is separated into several parts and the current is measured respectively. The current testing result is tabulated in Table 2.7.1.

Power down mode CC1000(only CC1000)	$\leq 3\mu A$
MCU LPM4(only MCU)	$\leq 1\mu A$
MCU LPM3(only MCU)	$\leq 4\mu A$
MCU LPM2(only MCU)	$\leq 76\mu A$
MCU LPM1(only MCU)	$\leq 361\mu A$
Active MCU(only MCU) with 3.3MHz clock	$\leq 1.490mA$
Active CC1000(only CC1000) RX	$\leq 12mA$
Active CC1000(only CC1000) TX	$\leq 27.8mA$

Table 2.7.1 Static Current Consumption of a Tag

Every day's average current consumption of a tag can be calculated according to Table 2.7.1.

$$\begin{aligned}
 \text{Current Consumption} &= (0.005s \times 13.5mA + 0.0035s \times 13.5mA + (2.5 - 0.005)s \times 0.007mA) \\
 &\quad \times \frac{24 \times 60 \times 60}{(2.5s + 0.0035s)} \\
 &= 4562.4mAs / day
 \end{aligned}$$

The rated capacitor of tag's battery is 1650mAh. So a tag using this battery can last:

$$\text{Total days} = \frac{1650mA * 60 * 60s}{4562.4mAs / day} = 1300day$$

The communication distance is measured in a sports field. A reader is put on a 3 meters high place and tags are put on a 1 meter high place. From testing result (see Table 2.7.2) we find that reader can correctly collect tags ID beyond 100meter. Thus

the communication distance is more than 100 meters.

Distance	Success/Fail
5m	Success
15m	Success
20m	Success
25m	Success
30m	Success
40m	Success
45m	Success
55m	Success
65m	Success
75m	Success
85m	Success
95	Success
100m	Success
110m	Success

Table 2.7.2 Communication Distance Testing

Photos of readers and tags are shown in Figure 2.7.1, Figure 2.7.2 and Figure 2.7.3.

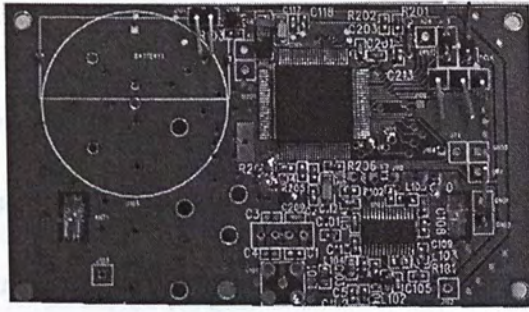


Figure 2.7.1 Top view of a tag

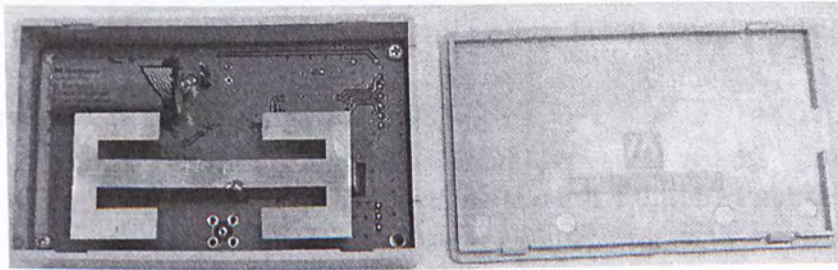


Figure 2.7.2 Bottom view of a tag



Figure 2.7.3 Top view of a reader

Reference:

- [1] *SP6201 Micropower, 100mA and 200mA CMOS LDO Regulators*
- [2] *ER14335 Lithium-thionyl Chloride Battery*
- [3] *ISO18000-7 Parameters for active air interface communications at 433MHz*
- [4] *MSP430F449 Specifications*
- [5] *CC1000 Single Chip Very Low Power RF Transceiver*
- [6] Lin.S. and D.J.Cosstelo. Jr. *Error control coding: Fundamentals and applications*,
Englewood Cliffs, NJ: prence Hall,1983
- [7] John G.Proakis, *Digital Communications* (Fourth Edition) Publish House of
Electronics Industry 2003

Chapter

3

Novel Power Saving Methods for an Active RFID System

3.1 Some drawbacks of the existing Active RFID protocol

In chapter 2 we described the whole implementation procedure of an active RFID system. This active RFID system complies with the ISO18000-7 protocol which is the only available active RFID protocol. Although it is the only available active RFID protocol it still has lots of unreasonable aspects. These unreasonable specifications are mainly focused on three aspects. The following sections will discuss these in detail.

3.1.1 Power consumption problem

In ISO18000-7 protocol, there are two fatal flaws which will cause very large power consumption. To reveal these flaws of the protocol we should analyze the wake up strategy of ISO18000-7 again. The wake up sequence of ISO18000-7 is shown in Figure 3.1.1.1.

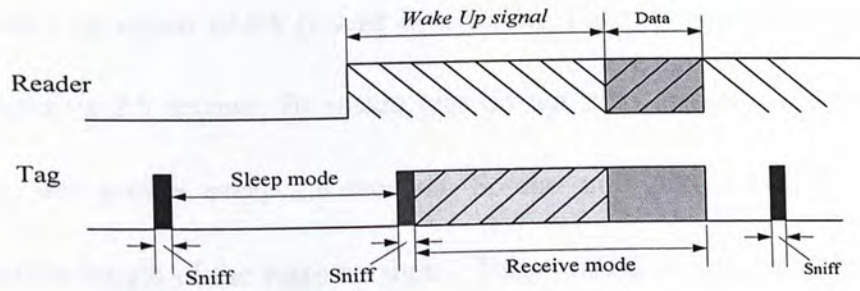


Figure 3.1.1.1 Wake up Sequence

To save power, a rudimentary method is to minimize the active time of a tag [1]. Thus, in a practical active RFID implementation, most of time tags will stay in sleep mode. Only when a reader sends a wake up signal to a group of tags, they will be woken after detecting this wake up signal. This kind of wake up strategy is used in ISO18000-7. In the upper side of Figure 3.1.1.1 we note that a reader will send out a wake up signal lasting for certain time which is specified to 2.5 seconds in this protocol. As we already described in Chapter 2, the wake up signal is a 30 KHz single tone sub-carrier which is near the operating center frequency. The maximum EIRP is 5.6 dBm which is already specified in ISO18000-7. After sending this single tone sub-carrier wake up signal, the reader will immediately send out a *Collection* command (most of time) or some other commands which is represented by blue color in Figure 3.1.1.1. However, how does a tag which is in sleep mode recognize that a reader send out a command and try to communicate with tags. For this consideration, most of time tags are in sleep mode and they will periodically awake and sniff all signals in the space in a certain operating frequency. Sniff activity means that a tag is in receiving mode and try to capture a *Wake Up* signal

which is sent by a reader. The wake up period of a tag is determined by the lasting time of a wake up signal which is sent by a reader. For instance, the length of a wake up signal is 2.5 second. To ensure tags do not miss any possible wake up signal, they will awake every 2.5 seconds. So the sniff period is 2.5 seconds according to the length of the wake up signal. These sniff activities are represented by blue blocks and red blocks in the lower part of Figure 3.1.1.1. The red block means that a tag successfully captures a valid wake up signal which is sent by a reader.

After capturing the wake up signal the tag will maintain receiving mode and wait for valid commands. These two stages are shown in the lower part of Figure 3.1.1.1 using a yellow block and a blue block. Tags will return to periodically sniff mode and try to catch other valid wake up signal after data transfer between tags and readers.

From the above sequence analysis we should clearly find out two disadvantages of this kind of wake up strategy. First of all, a single tone sub-carrier wake up signal is too simple so that tags will be easily woken by some fake wake up signals which actually are a very weak interference. We will try to figure out how weak is the interference can still wake up a tag.

According to the previous requirement analysis (see Chapter 2), the communication

distance is up to 100 meter. The transmission path between the transmitter and receiver always varies. Most of time, the Line-Of-Sight (LOS) electromagnetic propagation path does not exist. The signal path will be obstructed by buildings or large size object such as metal containers. Thus we should not use LOS model to estimate the communication distance and sensitivity of receiver. At this stage we do not have a particular model for a container yard. So we choose Hata model, which is one of the most widely used models for signal prediction in urban areas [2], to describe a container yard. The Hata model is an empirical formulation of the graphical path loss data provided by Okumura, and is valid from 150 MHz to 1500 MHz. It presented the urban area propagation loss as a standard formula which is given by:

$$PL(urban)(dB) = 69.55 + 26.16 * \log f_c - 13.82 * \log h_{te} - a(h_{re}) + (44.9 - 6.55 * \log h_{te}) * \log d \quad (3.1.1.1)$$

For a large city $a(h_{re})$ is:

$$a(h_{re}) = 3.2 * (\log 11.75 h_{re})^2 - 4.97 \text{ dB} \quad \text{for } f_c \geq 300 \text{ MHz} \quad (3.1.1.2)$$

Where f_c is the frequency (in MHz) from 150 MHz to 1500 MHz. h_{te} is the effective transmitter antenna height ranging from 30 meters to 200 meters. h_{re} is the effective receiver antenna height ranging from 1 meter to 10 meters. d (in km) is the distance between a transmitter and a receiver.

We assume the transmission antenna height is 100 meters and the receiver antenna height is 3 meters. So the propagation loss of the active RFID system is 116.75 dB when d is 1 kilometers. So far, we calculate the pass loss according to Hata model.

When the separation distance is 200 meters, this model is not suitable. However, both theoretical and measurement-based propagation models indicate that average received signal power decreases logarithmically with distance, whether in outdoor or indoor radio channels [2]. Thus the rough estimation of the Pass Loss of 100 meters in an urban area is

$$\begin{aligned} PL(100\text{meters}) &= PL(1\text{km}) - 20 \times \log\left(\frac{1\text{km}}{100\text{m}}\right) \\ &= 96.75\text{dB} \end{aligned} \tag{3.1.1.3}$$

In the above expression we only calculate the pass loss in an urban area. Moreover, we should consider the multipath fading effect. Multipath fading is caused by interference between two or more versions of the transmitted signal which arrive at the receiver at slightly different times [2]. Distortion of receiving signal will be occurred because of the severe multipath fading. Apparently multipath fading will affect the BER performance of the system.

First of all, we need to determine the type of fading in our application. We already assume the container yard environment is similar to an urban area when calculate the Pass Loss. Thus the RMS Delay Spread σ_r is $1.3\mu\text{s}$ [3]. The coherent bandwidth is:

$$B_c \approx \frac{1}{5 * \sigma_r} \tag{3.1.1.4}$$

B_c is 153.8 KHz. This coherent bandwidth is larger than our active RFID system bandwidth. So it is still flat fading. For coherent FSK the Probability of Bit Error

(for no ISI) in an AWGN channel is [4]:

$$P_B = Q\left(\sqrt{\frac{E_b}{N_0}}\right) \quad (3.1.1.5)$$

$\frac{E_b}{N_0}$ is equal to 10dB when P_B is an acceptable value (10^{-3}) for a normal digital

communication. However, considering the influence of flat fading the $\frac{E_b}{N_0}$ should

be much higher than 10 dB.

Secondly, we should also estimate whether the Doppler Shift which is caused by the movement of tags will affect the performance or not. The Doppler Shift is:

$$f_d = \frac{v}{\lambda} \cdot \cos \theta$$

In our case we assume the speed is 60km/h. Thus the maximum Doppler Shift f_m is 51 Hz. A popular rule of thumb for modern digital communication is to define the coherence time as:

$$T_c = \frac{0.423}{f_m}$$

So T_c is equal to 8.3×10^{-3} second. Thus the symbol rate of the active RFID system must exceed 120bits/s in order to avoid distortion due to frequency dispersion. Apparently, the symbol rate of the active RFID is much larger than 120bits/s. Therefore, this channel is a slow fading channel and it may be assumed to be static over one or several reciprocal bandwidth intervals.

From the above analysis we note that this channel is a flat fading and slow fading

channel. So we can use Rayleigh Fading Distribution, which is commonly used, to describe the statistically time varying nature of the received envelope of a flat fading signal. Compared with a typical FSK modulation performance in AWGN, the BER performance of FSK modulation in Rayleigh channel is much worst. When using FSK coherent detection and considering the Rayleigh channel fading, the $\frac{E_b}{N_0}$ is about 25dB [2]. The sensitivity of a receiver can be calculated as:

$$sensitivity = -174dBm + 10 * \log BW + NF + \frac{E_b}{N_0}$$

Where:

$\frac{E_b}{N_0}$ is equal to 25dB which is referred to Rayleigh channel fading

NF is Noise Factor

BW is System Bandwidth

From these calculations we know that the sensitivity of our active RFID receiver is -91dBm. Now the gain of receiver antenna is 5 dBi and the maximum EIRP from reader to tag is 5.6 dBm. The Pass Loss is 96.75 dB which we already calculate. So the signal strength is -86.15 dBm when it is 100 meters away from the transmitter and obviously it is still large enough for demodulated.

From the above analysis we set a signal strength threshold for all tags. A tag will be woken up only when the strength of wake up signal is larger than -90 dBm. The communication environment near 920MHz is severe. Lots of interference signals are larger than -90 dBm and some of them will last for a long time. If the

interference signals which are close to the operating frequency last more than 2.5 seconds, tags will treat them as a true wake up signal and wake up. This improper action will consume lots of power due to the fake wake up signals.

The second disadvantage of ISO 18000-7 is that a tag will averagely waste half of the wake up time for waiting a valid command which will be sent by a reader. For instance, if a wake up signal lasts 2.5 seconds, a tag will averagely waste 1.25 seconds when it is woken every time. This waiting time is represented by the yellow block in Figure 3.1.1.1. From Figure 3.1.1.1 we know that readers will immediately send out a command after sending a wake up signal. Tags will periodically sniff and try to get a valid wake up signal. However, tags will not know an accurate position within the wake up time when they successfully catch a wake up signal. Or we can simply say that the tag does not know how long it should wait for the first valid command which is sent by readers after capturing a wake up signal. So every time tags should maintain receive mode until it gets a valid command. If tags always stay in an area which is always having wake up signals, tags will continuously be woken up and maintain in receive mode for receiving a valid command even these tags are not supposed to have any operation. Unfortunately, for container yard management, most of time tags stay in the same place which is always covered by wake up signals. Batteries of these tags will be dissipated very soon under this kind of environment. So ISO18000-7 does not consider this kind of operation. This is the second disadvantage of this standard which will cause a big problem in power

consumption.

3.1.2 Multi-Reader problem

One fundamental application of an active RFID system is for long distance communications. The coverage of one reader is up to 100 meter. However, for container yard management, only one 100 meter is not enough. So we must increase the number of reader and try to cover much larger area. Then the Multi-Reader problem occurs. This is similar with GSM network. Both of GSM and active RFID have this kind of problem. A simple example is shown in Figure 3.1.2.1. In Figure 3.1.2.1 we note that there are two readers—reader A and reader B.

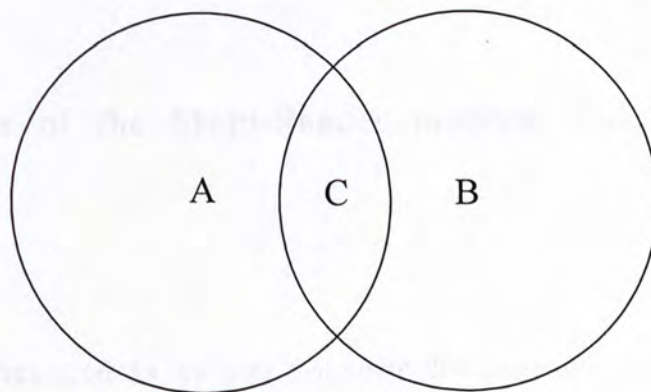


Figure 3.1.2.1 Two Areas with Overlap

The coverage area of Reader A and Reader B are $4\pi d^2$ because of the same sensitivity and output power. Apparently the overlap area—area C exists in the middle of the separation between Reader A and Reader B. If there are some tags stay in the overlap region C, they will receive the signal from Reader A and Reader B. Some problems will occur in this region. Let's assume that at the beginning a tag

detect a wake up signal from Reader A. Then the tag will try to communicate with Reader A. However, this tag also stays in the operating area which belongs to Reader B. So it also receives the signal which is sent by Reader B. It means the signal from Reader B becomes a strong interference signal when the tag is communicating with Reader A.

Moreover, the power consumption of tags will also increase when they stay in the overlap region. Tags in this region have more opportunity to be woken by different readers because they can receive wake up signals from both readers. Every time they will be woken and wait for a valid command after capturing a wake up signal. The ISO18000-7 protocol does not propose any solution for Multi-reader problem.

3.2 Solutions of the Multi-Reader problem and power saving problem

From the previous sections we note that some disadvantages exist in ISO18000-7 and these disadvantages make the standard unsuitable for container yard application. To solve the power consumption problems and Multi-reader problems we modify parts of the standard. Details will be presented in the following sections.

3.2.1 A solution to the power saving problem

As we already mention in Section 3.1.1 a wake up signal is a simple single tone sub-carrier which is close to the operating frequency. The sensitivity of receiver is about -90dBm to ensure long distance communication. So some very weak interference signals can wake up tags easily. To avoid interferences from fake wake up signal, we use modulated signal as a wake up signal instead of the simple single tone sub-carrier. Tags must demodulate the modulated wake-up signal and then identify whether this is a real wake-up signal or just an interference signal. However, what kind of information should we modulate into a wake-up signal?

In section 3.1.1 we mention that one drawback of ISO18000-7 is that tags do not know when the reader will begin to send commands after sending wake-up signal. So tags must maintain in receive mode and waste lots of power only for waiting. However, if we add certain time marker into every wake-up signal to create time stamp in a wake-up signal. When a tag captures a modulated wake-up signal, it will rapidly know when the reader will begin to send the valid data. After knowing the exact length of the time, the tag will get into a sleep mode and automatically wake up when the reader begins to send valid data. This modulated time marker wake-up scheme is illustrated in Figure 3.2.1.1.

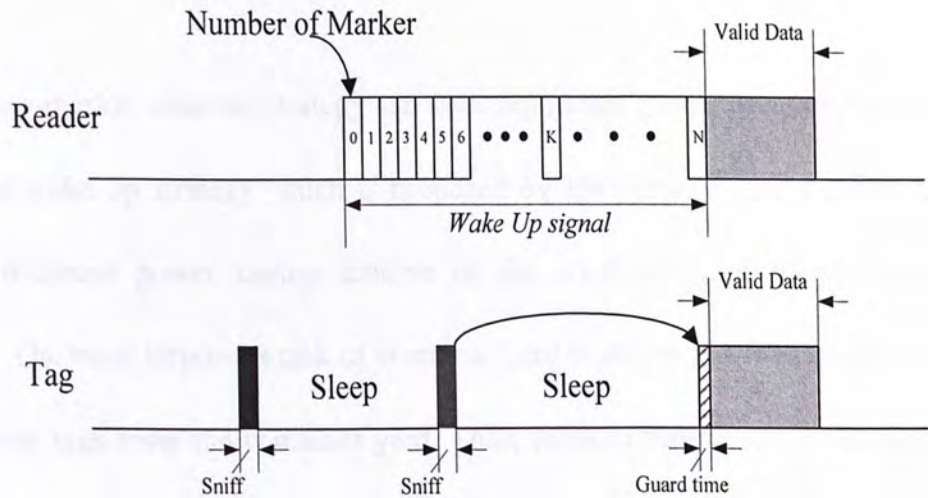
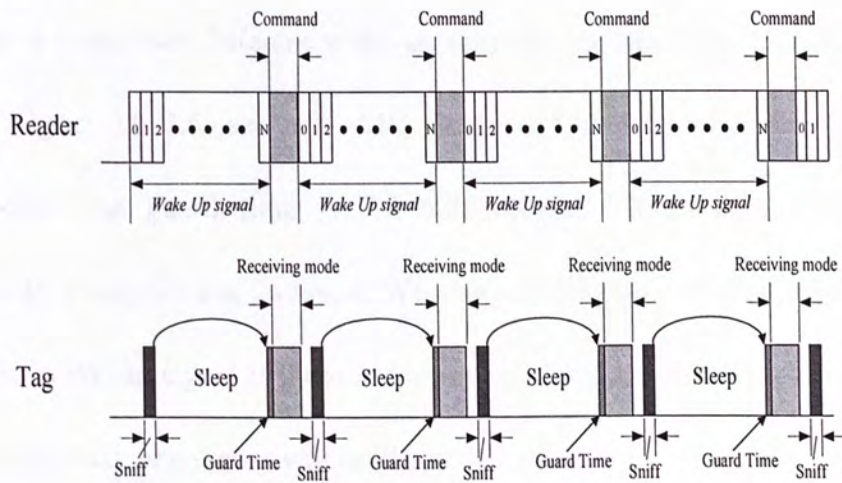


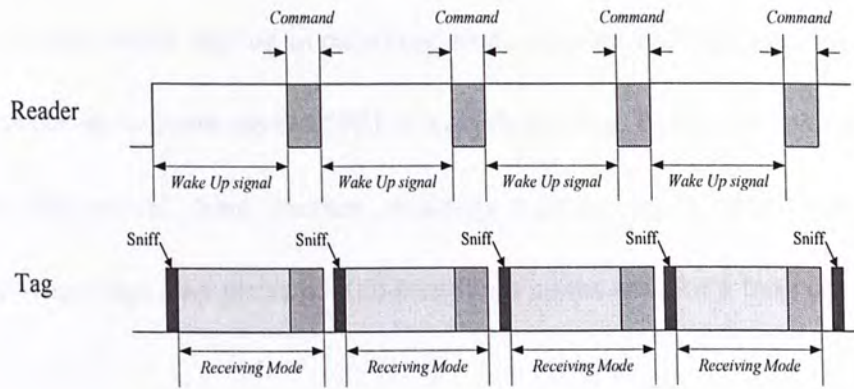
Figure 3.2.1.1 Time Sequence Diagram of the Modulated Time Marker Wake-up Scheme

From Figure 3.2.1.1 we note that this modulated wake-up signal is more complicated than the original wake up scheme which is proposed by ISO18000-7. Now the wake-up signal is not just a single tone sub-carrier. Before sending a valid data, reader will send the modulated wake-up signal that contains time marker number from Marker 0 to Marker N. Tags will periodically sniff the wake-up signal. In Figure 3.2.1.1 the red pulse refers the scenario in which the tag has successfully captured the modulated wake-up signal and extracted the time marker, say marker k, at the same time. If the total number of time marker is N, by simple calculation, the tag can easily find that the reader will start sending the valid data after $(N-K) \times \Delta T$. Thus, the tag will get into a sleep mode in this time interval. When $[(N-K) \times \Delta T - \text{Guard Time}]$ time pass, the tag will be woken up by itself and turn to the receiving mode to receive valid commands. Every time when a tag changes among sleep mode, transmitting mode and receiving mode, it needs to reserve some guard time to ensure the function in the tag is stable.

This new time-marker wake up strategy can save significant power when compared with the old wake up strategy which is proposed by ISO18000-7. Let's compare these two different power saving scheme in the container yard management application. The most important task of container yard management is to collect all tags' ID when tags enter the container yard. Thus, most of time readers will send out wake-up signal following by collection commands. We firstly assume an extreme case that a reader sends out wake-up signal and collection command in a whole day. The whole procedure is illustrated in Figure 3.2.1.2.



(a)



(b)

Figure 3.2.1.2 Comparison between Two Wake-up Scheme (a) Wake-up Signal with Time Marker (b) Wake-up Signal without Time Marker information.

Both of the total length of the wake-up signal and the length of the collection command in these two different wake-up schemes are the same. The length of a wake-up signal is 2.5 seconds. The length of collection command is 3.5 milliseconds. The guard time is 2.5 milliseconds. The length of Sniff is 6 milliseconds. Everyday has 24 hours. We also assume tags can always successfully capture the wake-up signal if there is a wake-up signal existing in space. Thus, we find that every day one reader will send out:

$$Num(wake_up\ signal + command) / day = \frac{24 \times 60 \times 60}{2.5 + 3.5 \times 10^{-3}} \quad (3.2.1.1)$$

And the total time that a tag maintains receiving mode when using wake-up signal with time marker is:

$$Time(receiving\ Mode) / day = Num \times (Sniff\ time + Guard\ time + Receiving\ Data)$$

The total time of tags when staying in receiving mode using time markers wake-up scheme is 414 seconds per day. However, the total time of tags adopting single tone

wake-up scheme when staying in receiving mode is about 86365.5 seconds per day. The new wake-up scheme saves 85951.5 seconds per day. From this comparison we note that this novel time marker wake-up scheme saves significant energy especially when tags stay under a valid communications area for a long time.

This new wake-up scheme also saves significant energy for frequently used tags. For instance, if a tag will be used 100 times per day, this new wake-up scheme will averagely save around $100 \times 1.25 \text{ seconds}$ per day when compared with the old single tone wake-up signal scheme (see Figure 3.2.1.3).

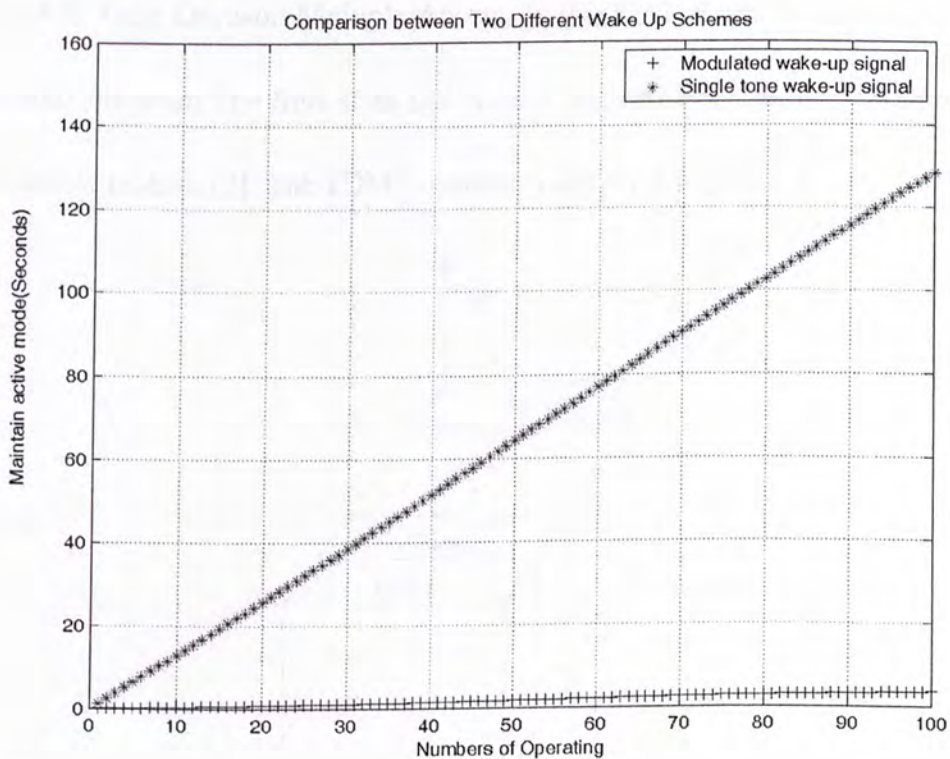


Figure 3.2.1.3 Comparison between Two different Wake-up Schemes under frequently operating of tags.

3.2.2 A solution to the Multi-Reader problem

We already know that Multi-reader problem exists in ISO18000-7. We have to adopt multi-reader to solve the large area coverage problem. Usually there are three kinds of multiple access techniques for wireless communications—TDMA, FDMA and SSMA. Finally we adopt FDMA in the active RFID system to solve the Multi-reader problem. In the following sections we will try to explain why we choose FDMA instead of TDMA and SSMA multiple access techniques.

TDMA is Time Division Multiple Access. In this kind of access method, it divides the radio spectrum into time slots and in each slot only one user is allowed to either transmit or receive [2]. The TDMA scheme is shown in Figure 3.2.2.1.

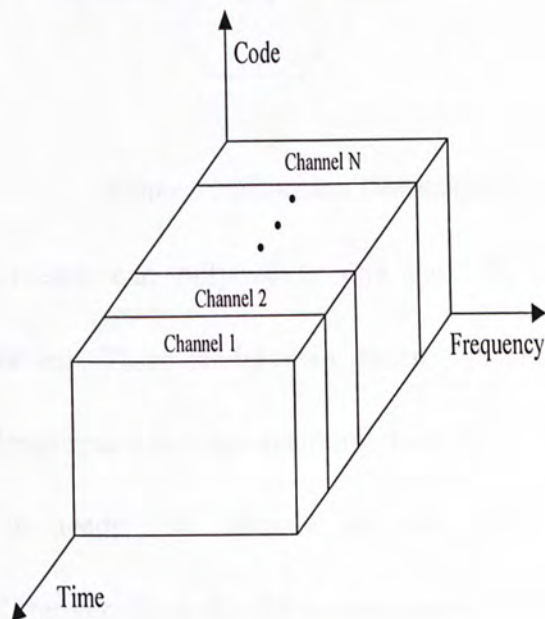


Figure 3.2.2.1 TDMA Scheme

If the TDMA Scheme is adopted in the active RFID system, it implies all readers must be accurately synchronized. However, in our active RFID system, readers can not communicate with each other. The only way of synchronized all readers is through intranet. But this kind of synchronization has large time delay. Another problem of adopting TDMA is the system efficiency problem. Let's assume readers are already synchronized and they are distributed as a honeycomb structure. It is illustrated in Figure 3.2.2.2.

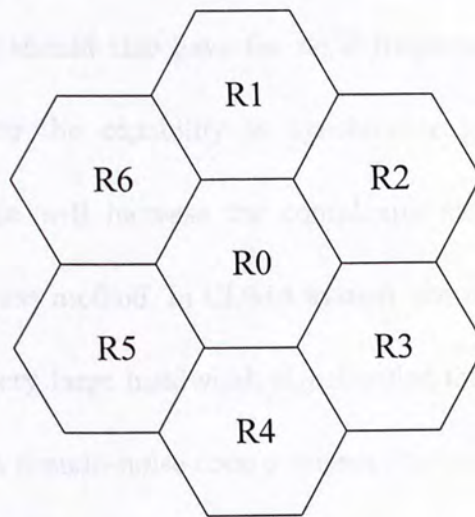


Figure 3.2.2.2 Reader Distribution Scheme

We assume every reader can only cover one cell. R0 is a reader which is surrounded by 6 readers. Three readers can transmit or receive in the same time slot because of the large space separation among them. Every time slot is at least 2.6 seconds so that it needs 7.8 seconds for all readers to complete their communications. Moreover, if reader R0 is communicating with tags in one time slot, all other readers must keep silence. Obviously the system efficiency becomes lower when using TDMA. Thus we do not adopt TDMA technology.

SSMA is Spread Spectrum Multiple Access. It includes two different access technologies. One is FHMA—Frequency Hopped Multiple Access another one is CDMA—Code Division Multiple Access. FHMA is a digital multiple access system in which the carrier frequencies of the individual users are varied in a pseudorandom fashion within a wideband channel [2]. FHMA is different as a FDMA system because the carrier frequencies change more rapidly. If readers are FHMA system, tags should also have the rapid frequency hopping capability and receiver should have the capability to synchronize its carrier frequency with transmitter. All these will increase the complexity and costs of tags. Thus we abandon FHMA access method. In CDMA system, the narrowband message signal is multiplied by a very large bandwidth signal called the spreading signal [2]. The spreading signal is a pseudo-noise code sequence. Inside a CDMA system, all users use the same frequency but each of them has their own pseudorandom codeword which is approximately orthogonal to all other codeword. A receiver performs a time correlation operation to detect only the specific desired codeword. However, CDMA needs a large bandwidth and tags must perform decorrelation. All these need the support from IC design especially for tags implementation. Another problem is that spreading the bandwidth will decrease the communication distance due to the increasing of system bandwidth. Thus we do not adopt CDMA multiple access method.

From the previous analysis we find that FDMA is the only choice and fortunately the FDMA are suitable and realizable for a low cost, practical active RFID system. FDMA is Frequency Division Multiple Access. FDMA assigns individual channels to individual users. So Readers are distributed as a honeycomb structure which is shown in Figure 3.2.2.3. Every seven readers will be composed as a cluster and each reader will be assigned a unique frequency. Thus a cluster has seven different frequencies. The frequency can be reused in other clusters. To decrease the adjacent channel interference, the frequency separation is 400 kHz.

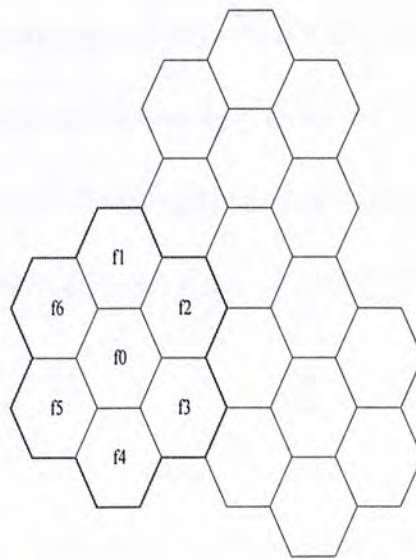


Figure 3.2.2.3 FDMA Scheme

Each cell can work independently due to the difference of frequency. Thus the system efficiency will not decrease. Every reader will continuously send out a modulated wake-up signal following by a collection command if it does not need to read from or write to a certain tag. This continuous wake-up signal is to make sure the reader will not miss any possible tag which is enter this cell. For instance,

when tags enter Cell 0 which is using frequency f_0 , they do not know which frequency is used. If tags do not get the correct frequency information they can not communicate with a reader. To solve this problem, tags will sweep every possible channel when they work in sniff mode. After sweeping different channel tags know which channel has the strongest signal. If the strength of the signal is larger than the threshold that we already set, this channel will be consider as a valid channel and tags will stay in this channel until the communication is failed certain times. Then tags will sweep different channel again until it gets a valid channel information. FDMA multiple access method does not have very high hardware requirements on tags. So it will not cause any cost increase of tags. And it also will not lower down the system efficiency. Thus finally we choose FDMA to solve the Multi-Reader problem. Experimental result shows that three readers can work in the same region without disturbing each other and tags can switch smoothly between these three readers.

Reference

- [1] Novel Power Saving Schemes for Active RFID System Implementation.
- [2] Theodore S.Rappaport *Wireless Communications Principles and Practice*,
Second Edition. Prentice Hall,Inc. 1996
- [3] 郭梯云 邬国扬 李建东 *移动通讯* 西安电子科技大学出版社. 1995
- [4] Bernard Sklar, *Digital Communication Fundamentals and Applications*,
Prentice-Hall (UK) Limited, 1988

Chapter

4

A Probe-fed Compact Half-wave Length Dipole Antenna for Active RFID System

4.1 Requirement of an antenna for Active RFID system

Compared to other communication systems, the operating environment of an Active RFID system is much worse. Active tags will be attached to the items with different contents and different backgrounds. Thus the antennas for active tags should have the capability to adapt different environment especially a metallic background. Metal strongly affects the performance of antennas by shifting their working frequency and lowering the radiation efficiency. In our container management application, all tags will be attached to containers, most of which are metallic objects. To ensure a reliable communication, antennas should be less affective to these metallic objects.

In our active RFID system, the antenna should have at least 5 MHz bandwidth. This bandwidth is base on the allocation of spectrum which is specified by TELECOMMUNICATIONS AUTHORITY OF HONG KONG [1]. The RFID spectrum which is allocated by Hong Kong government is from 920 MHz to 925 MHz.

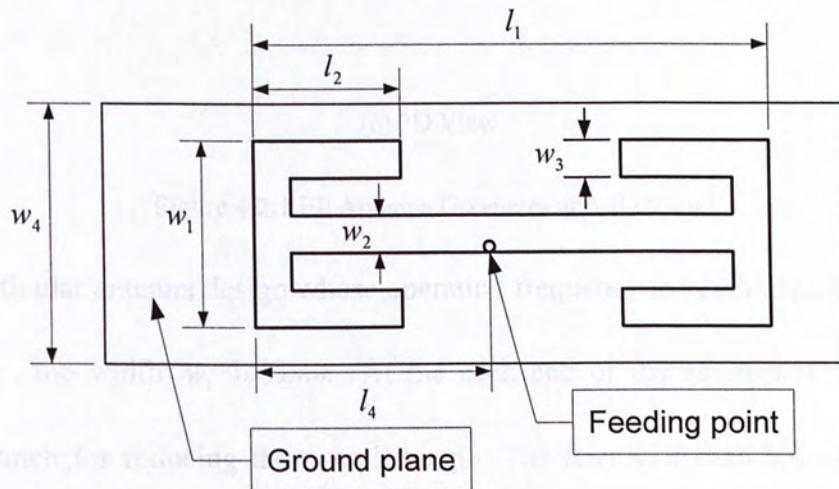
To save more power, the antenna gain needs to be around 5dBi. The EIRP which is specified by ISO18000-7 is 5.6dBm which is lower than the Hong Kong government's regulation [2]. From the consideration of the whole system performance, increasing the antenna gain will decrease the requirement of output power of tags. However, because of the limitation of the size of tags and the operating frequency, the antenna gain would not be too high.

4.2 A probe-fed half-wave length dipole EE shape antenna for metallic object application

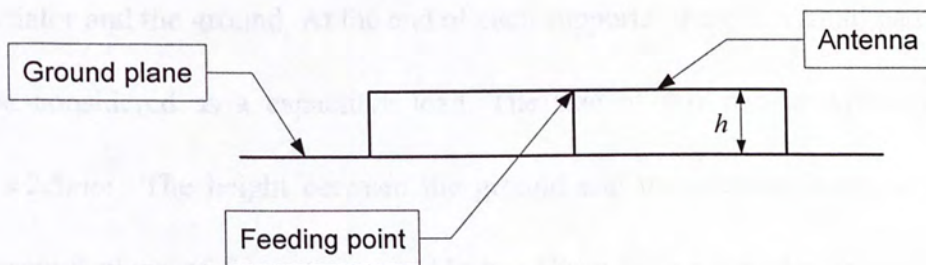
In this section, a novel EE shape antenna is proposed for active RFID systems, especially for some applications with metallic background such as container management. This EE shape antenna is a single-feed dipole antenna. It does not need a balun between the antenna and RF circuits. The operating frequency is easily tuned by changing the length of each branch of the antenna and the input impedance can be easily adjusted by moving the feeding point along the main trunk of the antenna. All these merits and the simplicity of the structure make it attractive for low cost, low profile compact tags.

To depress the influence of a metallic background, antennas which are omnidirectional should be avoided and, wherever possible, directional antenna should be

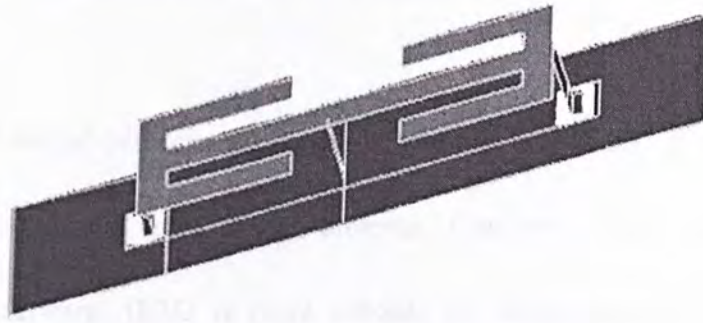
used because they have the advantage of fewer disturbances to the radiation pattern and to the return loss. From an antenna pattern we know that the EE shape antenna is a directional antenna. Moreover, we also find that the antenna gain does not change too much when a metallic background is close to the antenna. The geometry of this EE shape antenna is shown in Figure 4.2.1.



(a) Top View



(b) Side View



(c) 3D View

Figure 4.2.1 EE Antenna Geometry and 3D View

For a particular antenna design whose operating frequency is 920 MHz, the length l_1 is 68mm , the width w_1 is 31mm . At the each end of the antenna is an E letter shape branch for reducing the overall length. The length of each branch of the E letter can be changed according to different operating frequency. The length l_2 of this branch is 24mm for the particular design. There are two supporters between the radiator and the ground. At the end of each supporter there is a small pad, which can be considered as a capacitive load. The size of this pad is typically about $7\text{mm} \times 2.5\text{mm}$. The height between the ground and the antenna is about 10mm . The ground plane of the antenna is $115\text{mm} \times 36\text{mm}$ for a particular prototype. The width w_3 of each branch is 7mm . A feeding pin is directly connected to the antenna using a 10mm long and 1mm wide metal stripe. The position of this feeding pin can not be located at the center of the antenna because of the mismatch of input impedance. The length l_4 from one end to the feeding point is 31mm and from the other end to the feeding point is about 37mm for the same prototype.

4.3 Electromagnetic simulation results

We used Method-of-Moments-based electromagnetic-field solvers, IE3D, to simulate this single feed dipole antenna. Compared with other microwave simulation software, IE3D is more suitable for multi layer structure, not only because of its simulation speed, but also its accuracy in calculating an antenna pattern and frequency response. This antenna can be considered as a multi layer structure. One layer is the antenna and the other layer is the ground plane. The vertical structures are very simple and there is only a vertical metal stripe. In the IE3D simulation model, the highest meshing frequency is 2GHz with 20 cells per wavelength. In Figure 4.3.1 and Figure 4.3.2 are the Return Loss and Radiation pattern of the antenna.

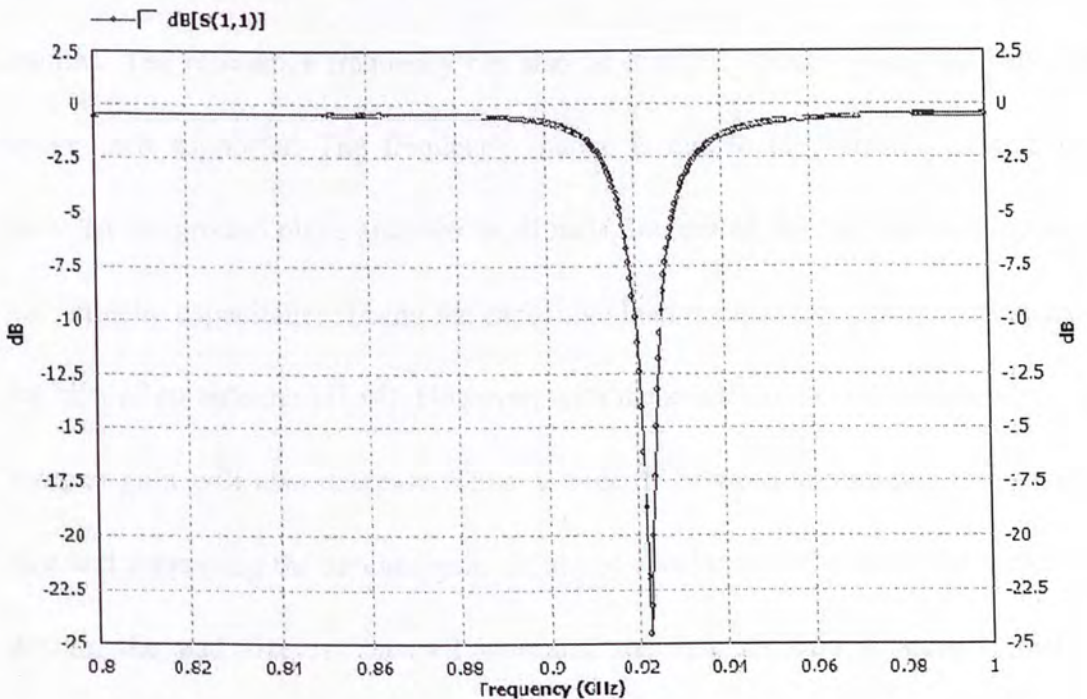


Figure 4.3.1 Return Loss of EE Antenna

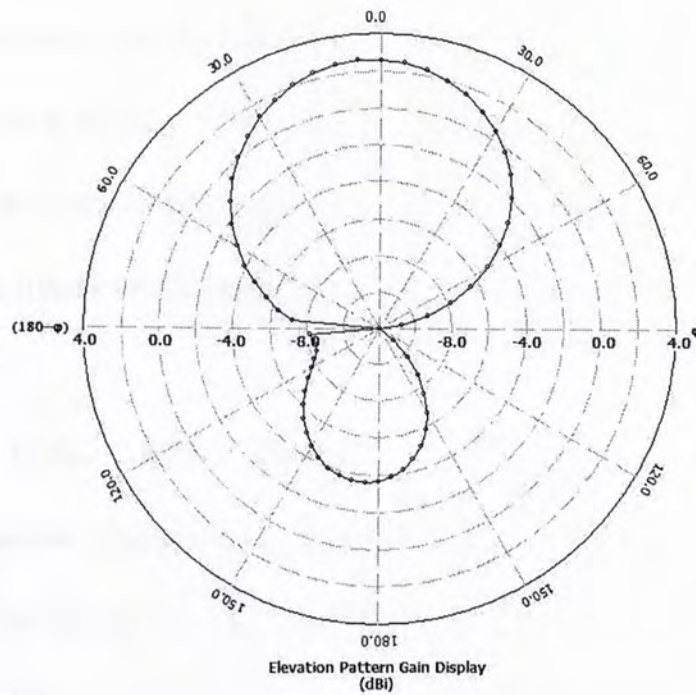
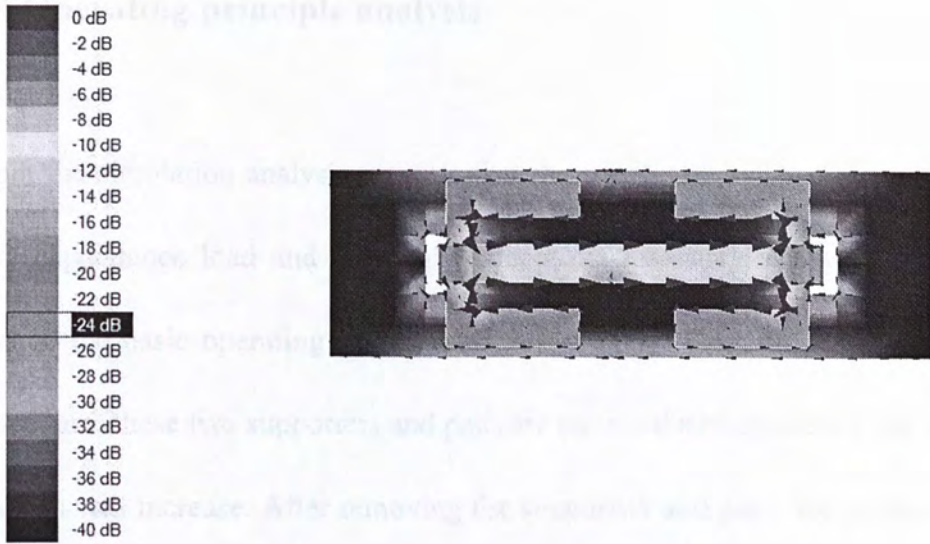


Figure 4.3.2 E Plane

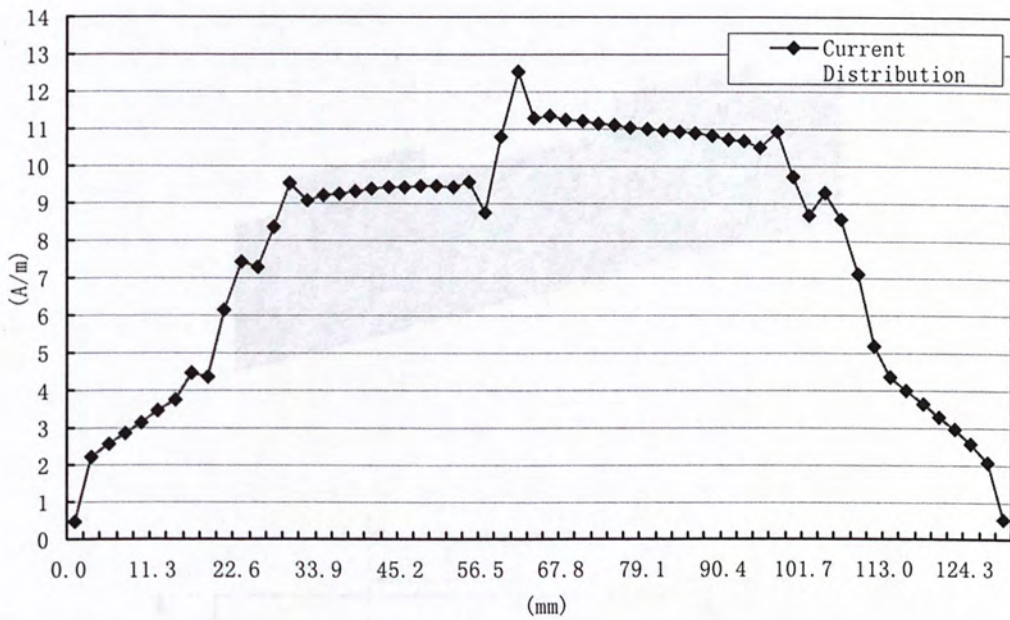
From Figure 4.3.1 we know the center frequency is 922.25MHz. The resonance frequency is determined by the total length of the antenna. However, the resonance frequency can be slightly adjusted by tuning the length of each branch of the antenna. The resonance frequency can also be changed through tuning the pad size under each supporter. The frequency change is due to the parasitic capacitance between the ground plane and two small pads. Increasing the pad size will increase the parasitic capacitance. Using the capacitive load method can significantly reduce the size of an antenna [3] [4]. However, with the minimization of antenna size, the antenna gain will also decrease. Thus, a tradeoff between minimizing the antenna size and increasing the antenna gain should be considered. In a particular prototype design, the pad size is $7mm \times 2.5mm$ and the antenna gain is around 4dBi in simulation result.

The input impedance of the antenna can be easily changed by changing the feeding pin position along the edge of the antenna. And resonance frequency does not shift a lot with the movement of the feeding pin. According to the above characteristics, the resonance frequency and input impedance can be tuned separately.

Figure 4.3.3 is the current distribution of an EE antenna. Usually a dipole is center-fed and the current vanishes at the end points. Experimentally it has been verified that the current in a center-fed wire antenna has sinusoidal form with null at the end point [4]. A current distribution of a small dipole which is shorter than half wavelength is a quasi sinusoidal form. From Figure 4.3.3 we find that the single-fed structure of this double E shape antenna also excites a quasi sinusoidal form current distribution. The current on the backbone of the antenna surface has the same direction. At the end of each branch the current is decreased to almost zero. The length of this antenna, including the length of each branch, is 94mm. It is shorter than half wavelength of 920 MHz and even close to quarter wavelength. Compared with normal dipole antenna, this single feed EE antenna does not need a differential input and also has the same performance.



(a) 3D View of the Current Distribution



(b) Current Distribution from The Left Side Branch to The Right Side Branch.

Figure 4.3.3 Current Distribution of EE Antenna

4.4 Operating principle analysis

From the simulation analysis we note that the supporters and the pads are working as a capacitance load and they only affects the resonate frequency. They do not change the basic operating principle of this antenna. Thus, to simply the analysis procedure, these two supporters and pads are removed and apparently the size of the antenna will increase. After removing the supporters and pads, the geometry of this antenna and 3D view is illustrated in Figure 4.4.1.

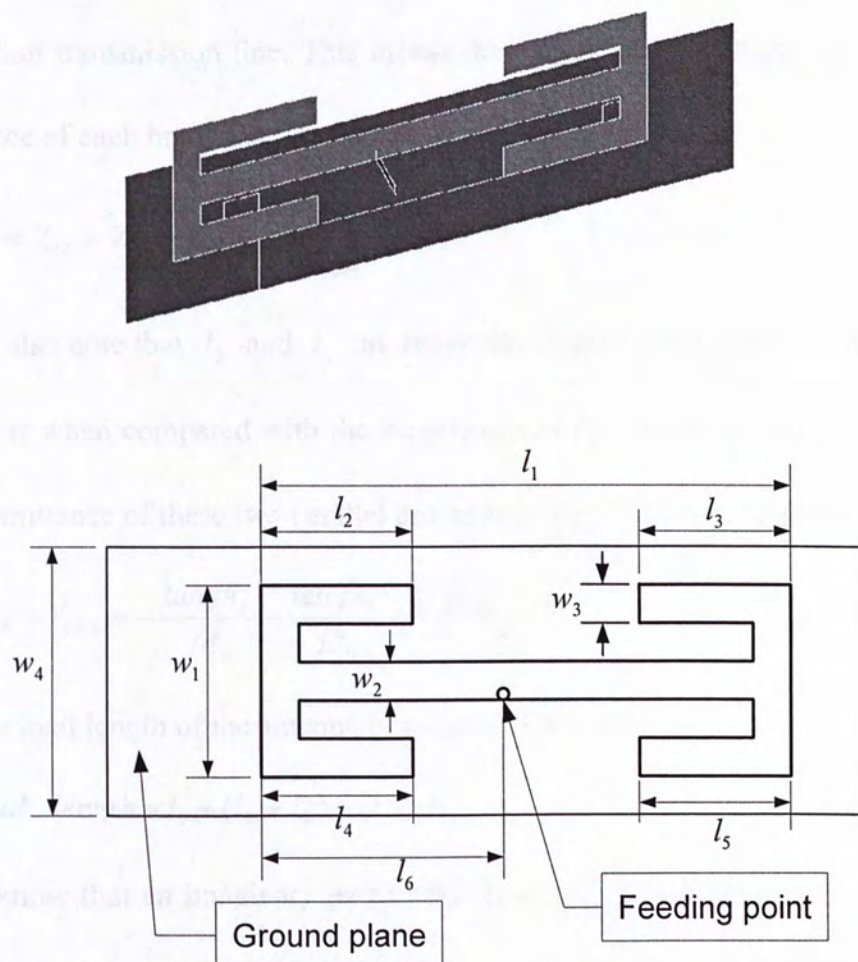


Figure 4.4.1 EE Antenna without supporters and pads

Compared with the EE shape antenna with supportors, this one is much longer and the length l_1 is $88mm$. The original length of l_1 is $68mm$. The length of l_2, l_3, l_4 and l_5 are all equal to $27mm$. First of all, we will investigate the resonance frequency of this antenna using transmission line model.

Firstly, we consider a lossless transmission line model to model the antenna. The formula for the input impedance of a lossless transmission line is [5]

$$Z_i = R_0 \frac{Z_L + jR_0 \tan \beta l}{R_0 + jZ_L \tan \beta l}$$

From Figure 4.4.1 we note that l_2, l_3, l_4 and l_5 can be treated as an open-circuit termination transmission line. This means the output load is infinite. So the input impedance of each branch is:

$$Z_{i5} = Z_{i2} = Z_{i3} = Z_{i4} = -\frac{jR_0}{\tan \beta l}$$

And we also note that l_2 and l_4 are in parallel to each other and both of them are very short when compared with the wavelength of the operating frequency. So the input admittance of these two parallel branches is approximately equal to:

$$Y_{i2/4} = Y_{i3/5} = -\frac{\tan \beta l_2}{jR_0} - \frac{\tan \beta l_4}{jR_0} \approx -\frac{\beta(l_2 + l_4)}{jR_0}$$

Thus the total length of the antenna is approximately equal to:

$$Total \ length = l_1 + (l_2 + l_4) + (l_3 + l_5)$$

We all know that an imaginary part of the input impedance is equal to zero when antennas begin to resonate. From transmission line theory we know that the input reactance is equal to zero when the length is half wavelength. Thus the

Total length of this antenna is approximately equal to $\lambda/2$. Secondly, we try to use lossy transmission line model to describe the radiation loss and the input impedance variation of the antenna due to the change of feeding position.

First of all, we use IE3D to simulate the change of input impedance according to different feeding position. The feeding position is moved from the left side (Point A) to the right side (Point I, see Figure 4.4.2). Point E is the matching point of the antenna. The interval between two points is 0.5mm . Figure 4.4.2 shows the different feeding positions of the antenna.

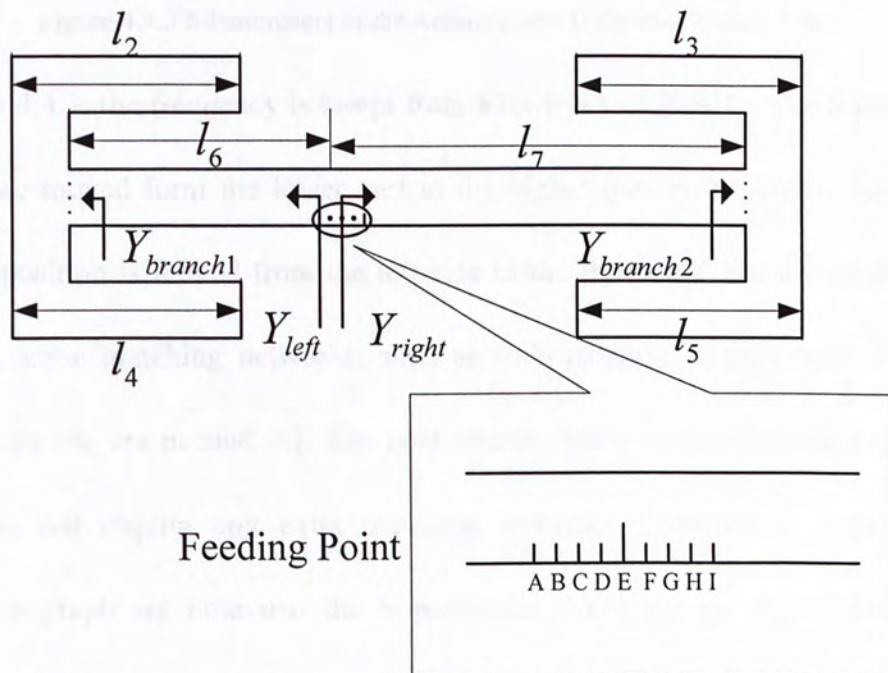


Figure 4.4.2 Different Feeding Positions

The different S11 parameters of this antenna with different feeding positions are shown in Figure 4.4.3.

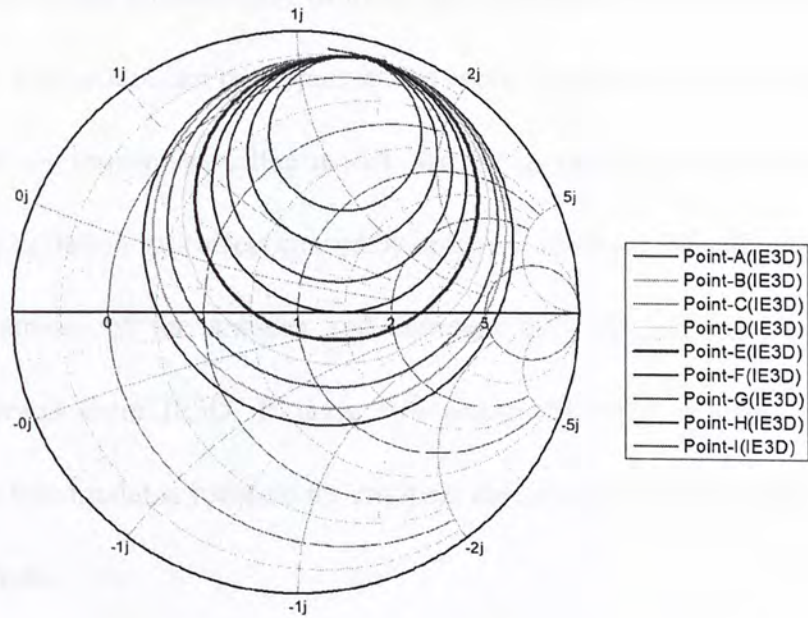


Figure 4.4.3 S Parameters of the Antenna with Different Feeding Point

In figure 4.4.3, the frequency is swept from 870MHz to 970MHz. The S parameter curves are moved from the lower part to the higher part in the smith chart when feeding position is moved from the left side to the right side. For a typical dipole antenna, some matching networks, such as stub-matching, transformer, T-match, Gamma match, are needed [6]. The new antenna has a simple matching structure and does not require any extra matching elements. Furthermore, from the S parameter graph we note that the S parameter curve change significantly with different feeding position. This significant change of S parameter makes us very convenient to adjust the input impedance without any complex matching circuits.

This antenna is suspended above a metallic ground. To study the input impedance of the antenna as a function of feeding position, we use a lossy transmission line

model to describe the characteristic of input impedance. Obviously an ideal lossless transmission line model can not represent the input S parameter of an antenna. So we choose lossy transmission line model. We try to use dielectric loss model to represent the radiation loss effect caused by antenna radiation. We will calculate the input S parameter of the antenna and compare the calculated result with the simulation result from IE3D. If these two results fit well, it means the lossy transmission line model is justified for studying the antenna input impedance vs the feeding position.

In a lossy transmission line model, the wave number is no longer a simple real value, but a complex number:

$$\varepsilon_c = \varepsilon' - j\varepsilon'' \quad (4.4.1)$$

The imaginary part of a complex permittivity ε_c includes both the radiation loss and conducting loss [7]. According to this complex permittivity, the wave number is change to a complex number:

$$k_c = \omega\sqrt{\mu\varepsilon_c} = \omega\sqrt{\mu(\varepsilon' - j\varepsilon'')} \quad (4.4.2)$$

From Figure 4.3.2 we note:

$$Y_{branch1} = Y_2 + Y_4 = -\frac{\tan k_c l_2}{jR_0} - \frac{\tan k_c l_4}{jR_0} \quad (4.4.3)$$

$$Y_{branch2} = Y_3 + Y_5 = -\frac{\tan k_c l_3}{jR_0} - \frac{\tan k_c l_5}{jR_0} \quad (4.4.4)$$

Two parallel branches, branch 1 and branch 2, are working as the load of the stripe 1

l_6 and l_7 , respectively. So the input admittance of two opposite sides, the left side and the right side which are shown in Figure 4.4.2, are:

$$Y_{left} = Y_0 \frac{Z_0 + jZ_{branch1} \tan k_c l_6}{Z_{branch1} + jZ_0 \tan k_c l_6} \quad (4.4.5)$$

$$Y_{right} = Y_0 \frac{Z_0 + jZ_{branch2} \tan k_c l_7}{Z_{branch2} + jZ_0 \tan k_c l_7} \quad (4.4.6)$$

Apparently, the input admittance of this antenna is the sum of left side input admittance and the right side admittance.

$$Y_{total} = Y_{left} + Y_{right} = Y_0 \left(\frac{Z_0 + jZ_{branch1} \tan k_c l_6}{Z_{branch1} + jZ_0 \tan k_c l_6} + \frac{Z_0 + jZ_{branch2} \tan k_c l_7}{Z_{branch2} + jZ_0 \tan k_c l_7} \right) \quad (4.4.7)$$

The input impedance is the reciprocal of Y_{total}

$$Z_{total} = 1/Y_{total} \quad (4.4.8)$$

However, inside the expression of Z_{total} , the characteristic impedance Z_0 and the complex wave number k_c are still unknown. To find out the exactly value of Z_0 and k_c , we simulate a finite length lossy transmission line. By assuming the loss tangent of this lossy model, we can extract the basic parameters of this particular transmission line. The height of the transmission line is the same as that of the antenna. The length of this transmission line is:

$$l_{trans-line} = l_6 + l_7 \quad (4.4.9)$$

The extracted basic parameter is shown in Table 4.4.1:

Freq(GHz)	Z_0 (Ohms)	Re(Ereff)	Im(Ereff)
0.92	173	1.00035	-0.00780152

Table 4.4.1 Basic Parameter of the Lossy Transmission Line

Substituting these values into expressions (4.4.7) and (4.4.8), one can find the real part and imaginary part of the input impedance, respectively for different feeding positions. The calculated results are shown in Figure 4.4.4 and Figure 4.4.5. The simulation result using IE3D is shown in Figure 4.4.6 and Figure 4.4.7

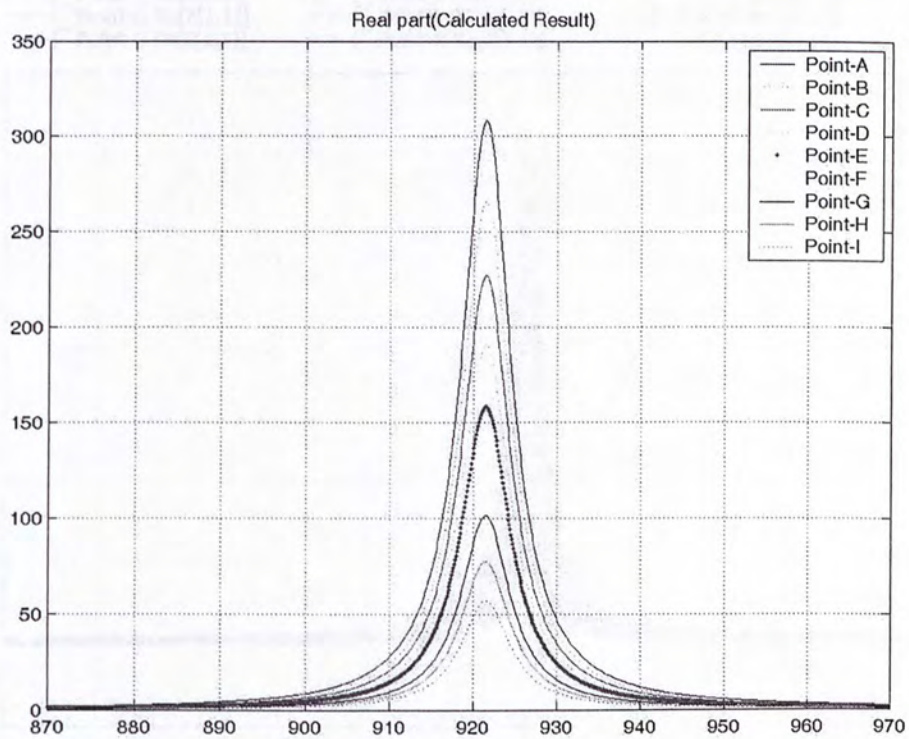


Figure 4.4.4 Real Part of input impedance from Lossy TLN Model

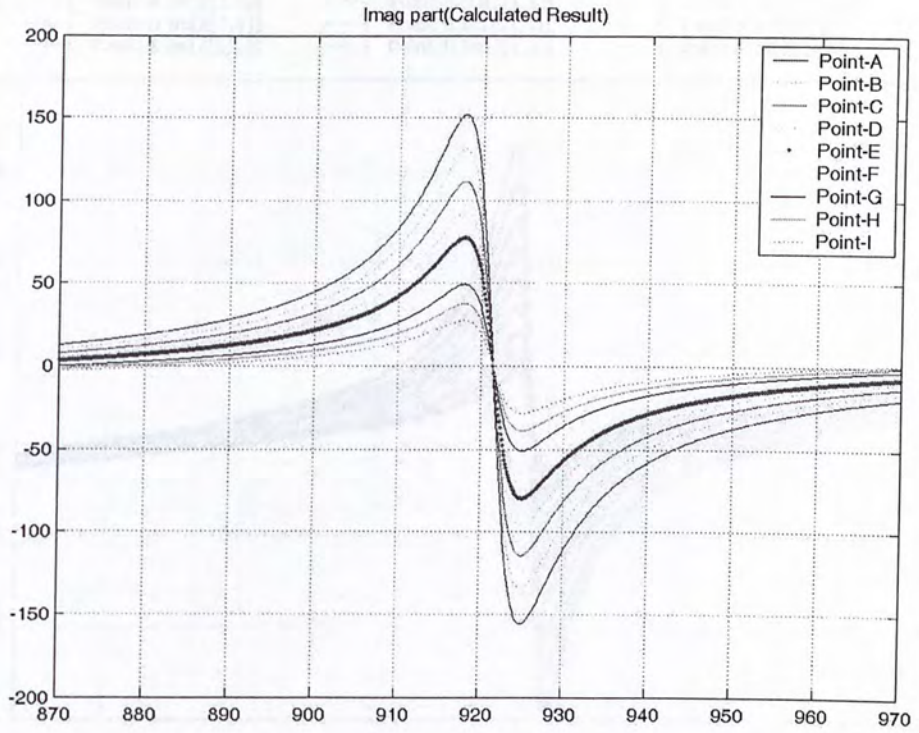


Figure 4.4.5 Imaginary Part of Input Impedance from Lossy TLN Model

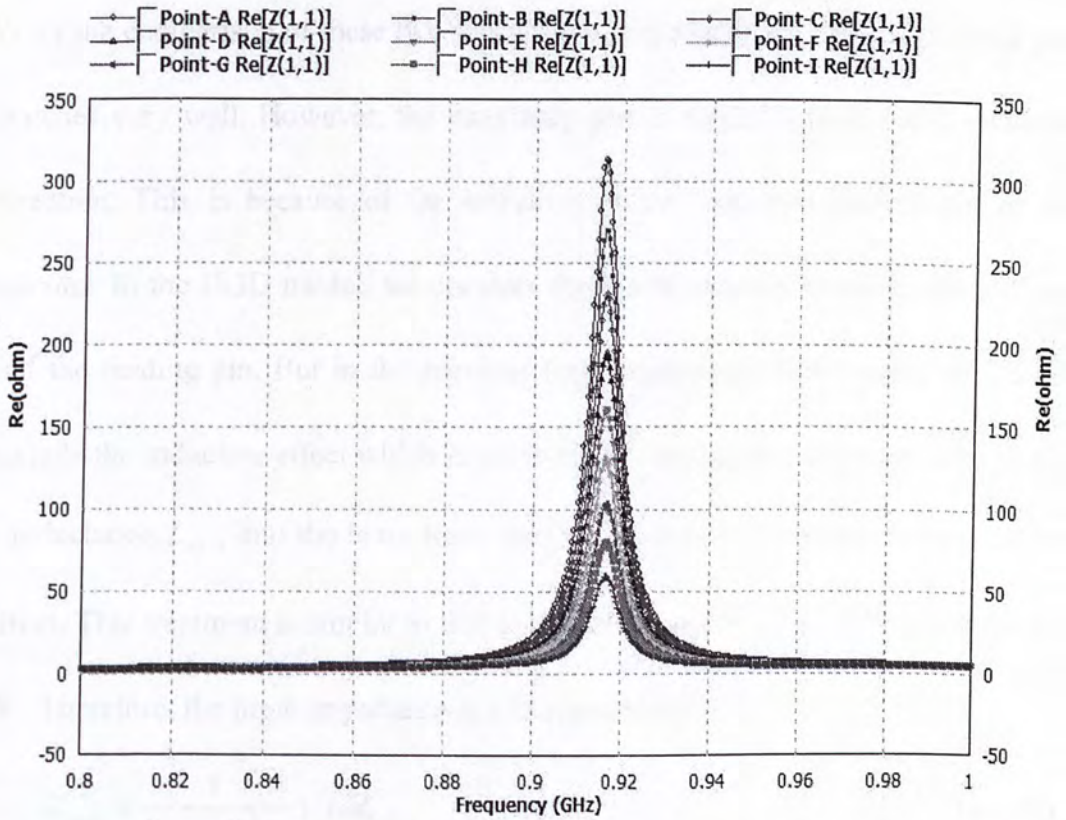


Figure 4.4.6 Real Part of Input Impedance from IE3D

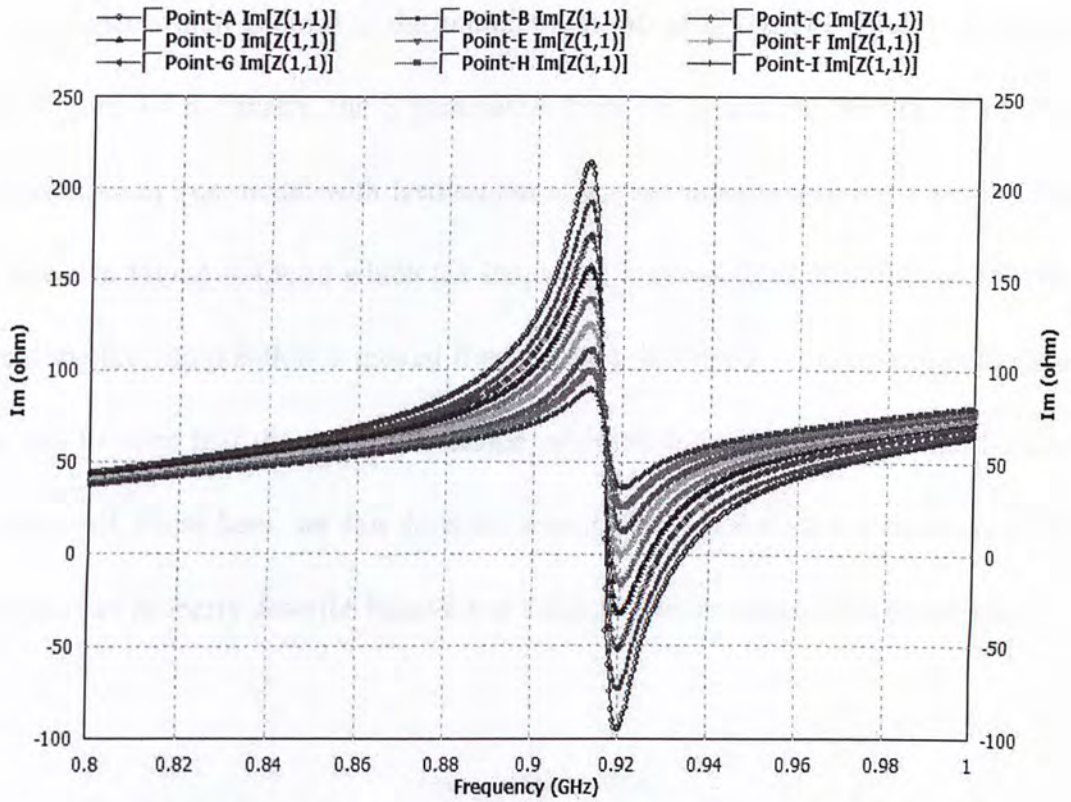


Figure 4.4.7 Imaginary Part of Input Impedance form IE3D

From the comparison of these two sets of input impedance we find that the real part matches very well. However, the imaginary part is shifted toward the capacitance direction. This is because of the influence of the inductive feeding pin of the antenna. In the IE3D model, we consider the whole antenna including the radiator and the feeding pin. But in the previous lossy transmission line model we do not include the inductive effect which is caused by the feeding pin. Thus we need to add an inductance, L_{eff} , into the lossy transmission line model to replace the feeding pin effect. This treatment is similar to that in the cavity model of microstrip antenna [8] [9]. Therefore, the input impedance can be represented by:

$$Z_{total} = \frac{1}{Y_{left} + Y_{right}} + j\omega L_{eff} \quad (4.4.10)$$

Using this expression we can finally get the reasonable imaginary part of the input

impedance which is close to the simulation result of IE3D. The result is illustrated in Figure 4.4.8. Finally, the S parameters from IE3D and the calculation of lossy transmission line model with feeding pin effect are superimposed in a Smith Chart shown in Figure 4.4.9, in which the frequency is swept from 900MHz to 940MHz and the feeding position is moved from Point-A to Point-I. From the Smith Chart it can be seen that the transmission line model match to the full wave EM model very well. From here, we can draw the conclusion that the lossy transmission line model can properly describe behavior of the input characteristic of this antenna.

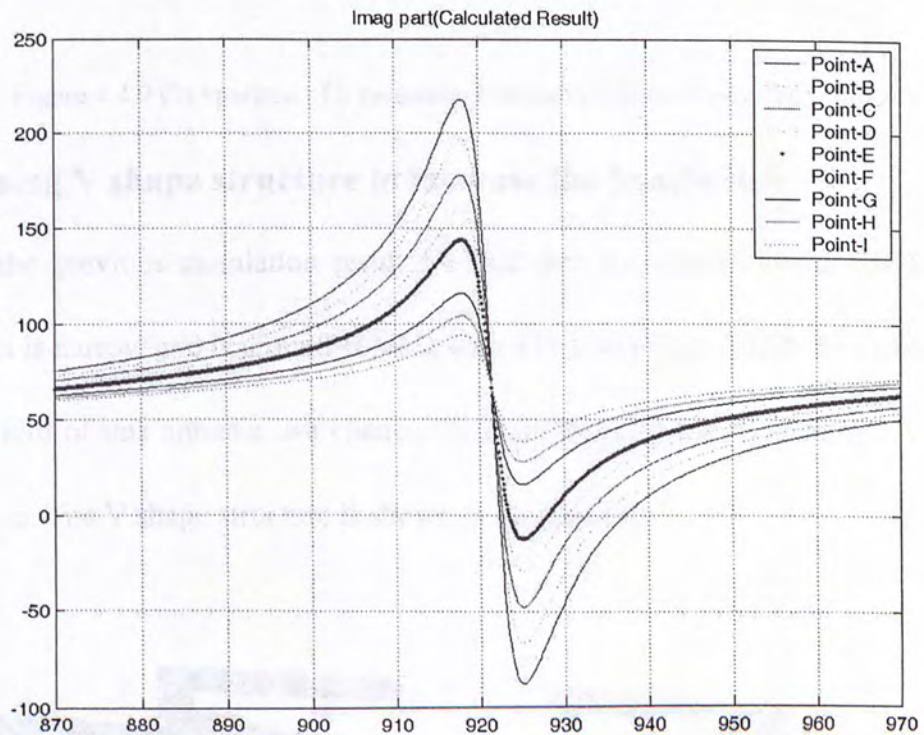


Figure 4.4.8 Imaginary Part with Feeding Pin Effect

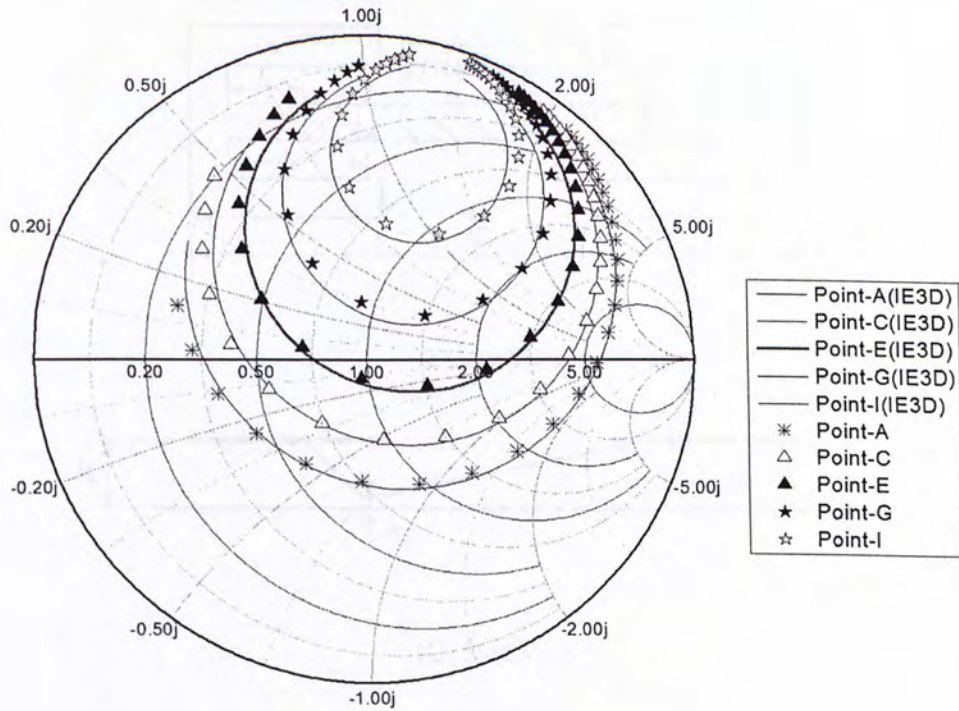
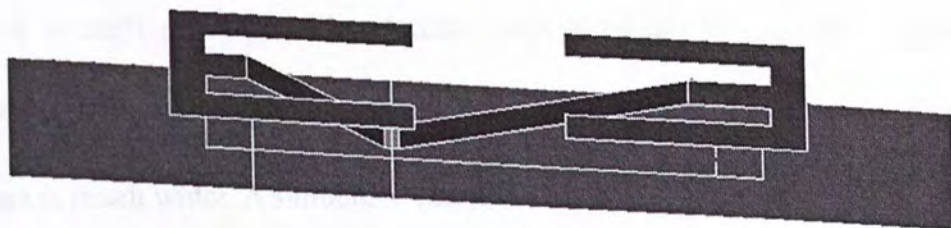


Figure 4.4.9 Comparison of S parameter between IE3D and Lossy TLN Model

4.5 Using V shape structure to increase the bandwidth

From the previous simulation result we find that the bandwidth of this kind of antenna is narrow and is around 10MHz with S11 lower than -10dB. To increase the bandwidth of this antenna, we change the main trunk of the antenna to a V shape structure. The V shape structure is shown in Figure4.5.1:



(a) 3D view

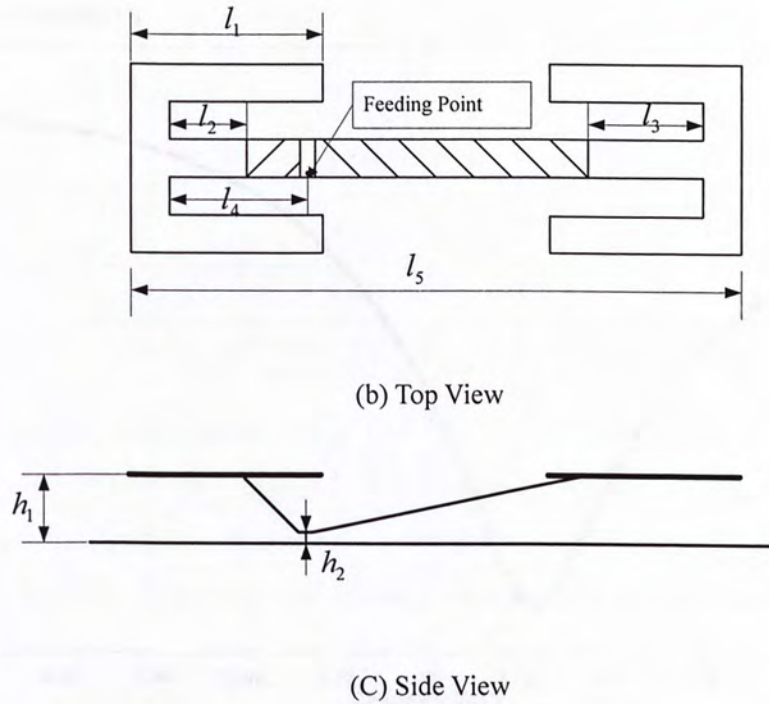


Figure 4.5.1 V Shape Structure Antenna

l_2 is 5.6mm. l_3 is 11.4mm. The backbone length l_3 is 88mm. h_2 is 2mm. The antenna can be easily matched by moving the feeding position along the main trunk. The input impedance of the original antenna without V shape structure is affected by the long feeding pin (10mm). A high inductance is induced by this long feeding pin. The capacitance between the V shape structure and the GND cancels the inductive effect and the V shape structure also acts as a matching network due to the gradual changing of the characteristic impedance of the antenna. Therefore, compared with the original antenna, the bandwidth of this V shape Structure antenna is much wider. A simulation result is shown in figure 4.5.2.

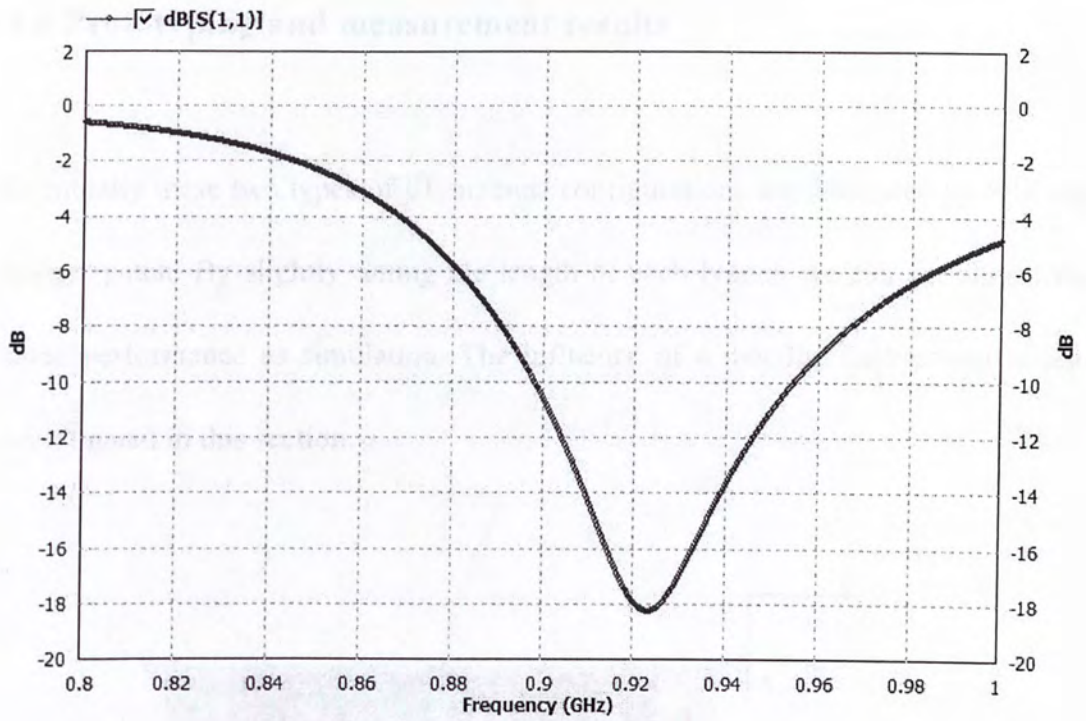


Figure 4.5.2 |S11| of the V Shape Structure Antenna

The bandwidth comparisons between the V shape structure antenna and the original one are tabulated in Table 4.5.1.

Bandwidth	-5dB	-10dB	-15dB
With V Shape structure	121MHz	56MHz	24MHz
Without V shape strucute	14MHz	9MHz	4MHz

Table 4.5.1 Comparison between the Antennas with and without V Shape Structure

Obviously, the V shape structure significantly increases the bandwidth.

4.6 Prototyping and measurement results

Eventually these two types of EE antenna configurations are fabricated by FR4 and copper patch. By slightly tuning the length of each branch we can get almost the same performance as simulation. The influence of a metallic background is also investigated in this section.

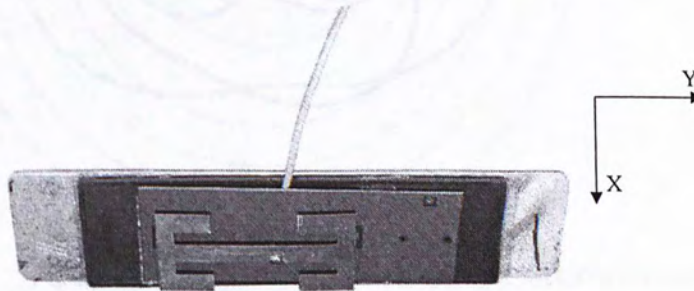


Figure 4.6.1 Original EE Antenna

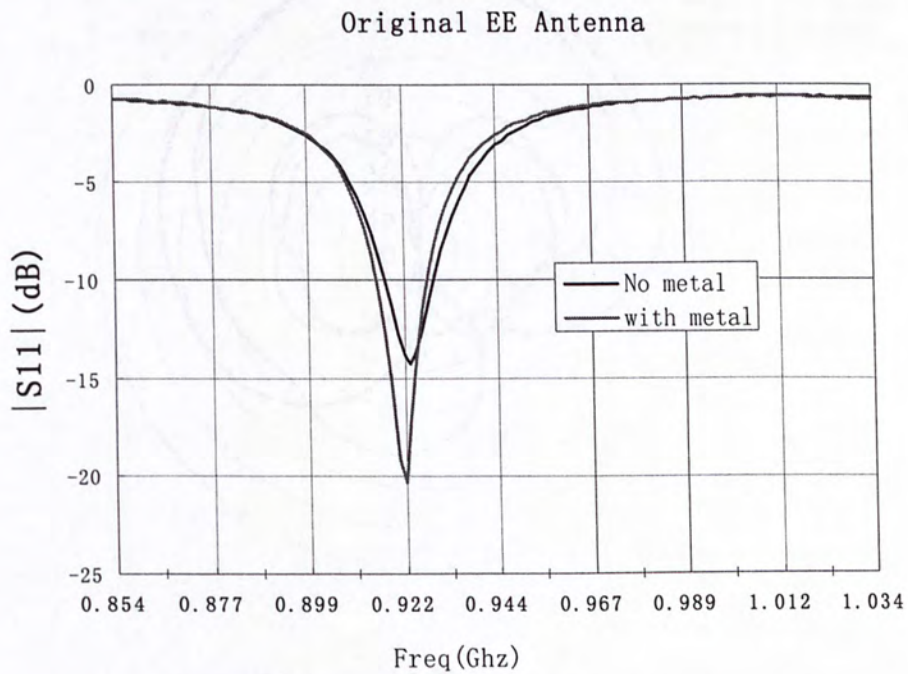


Figure 4.6.2 $|S_{11}|$ of Original EE Antenna without V shape structure.

Original EE Antenna(No Metal)

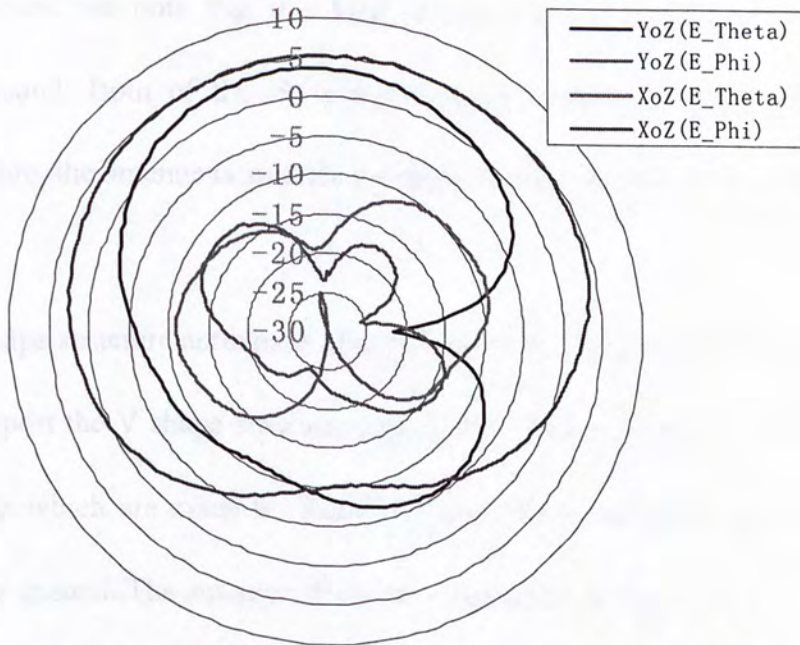


Figure 4.6.3 Original EE Antenna Without Metallic Background

Original EE Antenna(With Metal)

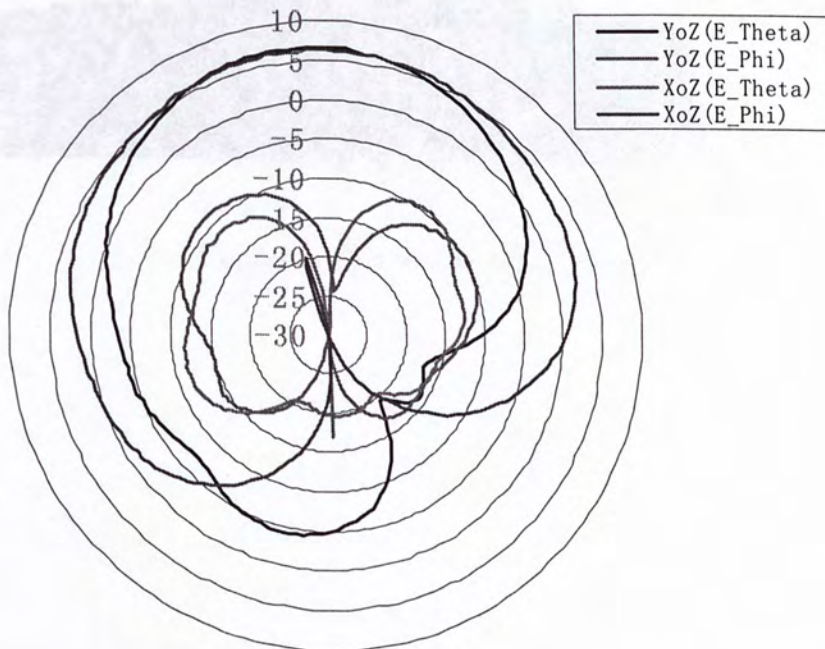


Figure 4.6.4 Original EE Antenna with Metallic Background

From the comparison between no metallic background and with metallic background we note that this kind of antenna is not sensitivity to the metallic background. Both of the $|S_{11}|$ and radiation pattern are only slightly changed. Therefore, the antenna is suitable for applications with metal environments.

A V shape structure antenna is also fabricated by using FR4 PCB and copper patch. To support the V shape structure and control the height above the PCB board, two cuboids which are made by foam are inserted into the space between the radiator and the ground. The antenna structure is illustrated in Figure 4.6.5.



Figure 4.6.5 V Shape Structure Antenna

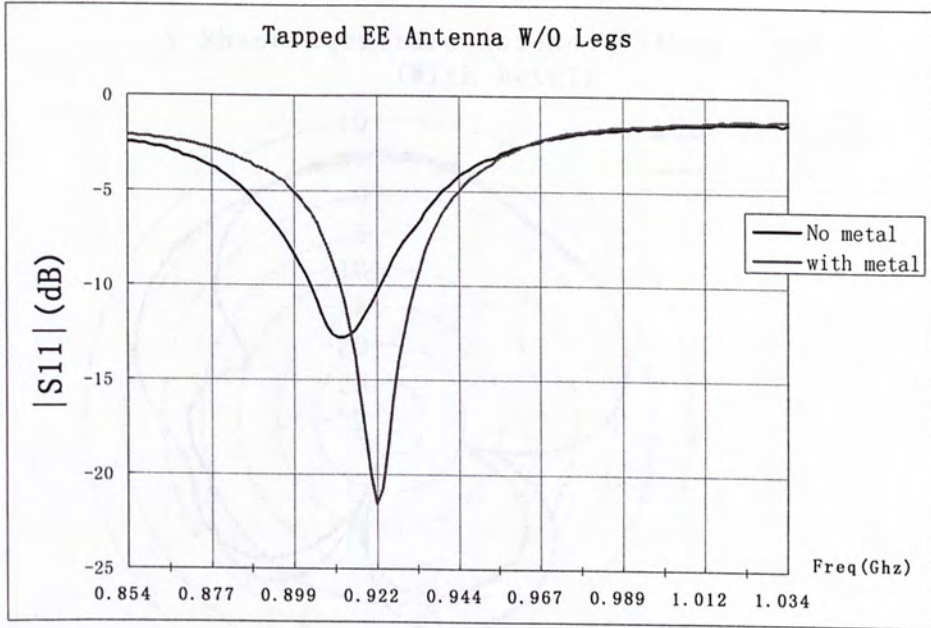


Figure 4.6.6 $|S_{11}|$ of V Shape Structure Antenna With and Without Metallic Background

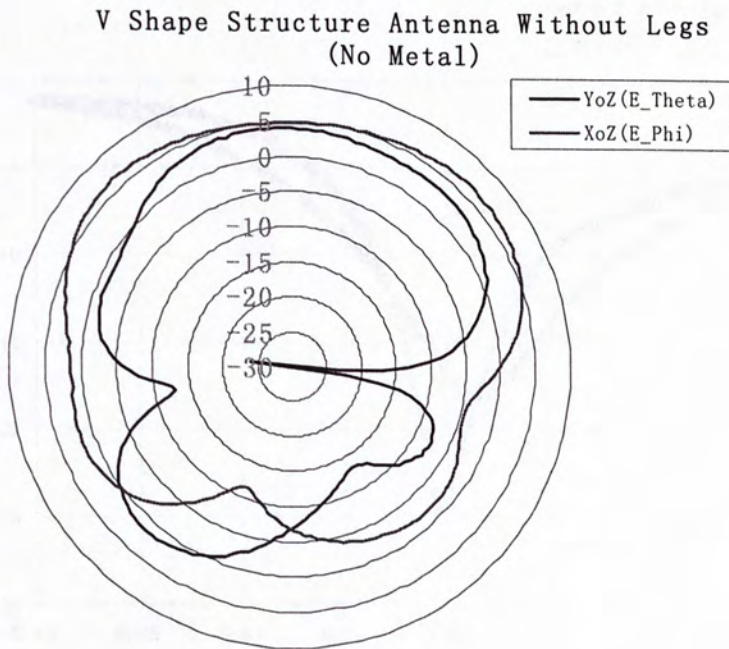


Figure 4.6.7 Radiation Pattern of V Shape Structure Antenna Without Legs

V Shape Structure Antenna Without Legs
(With Metal)

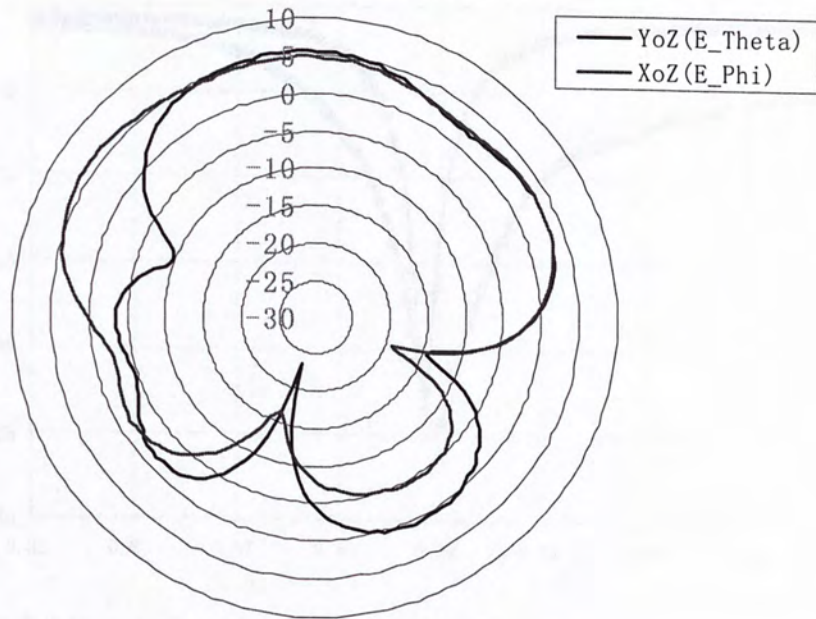


Figure 4.6.7 V Shape Antenna With Metallic Background

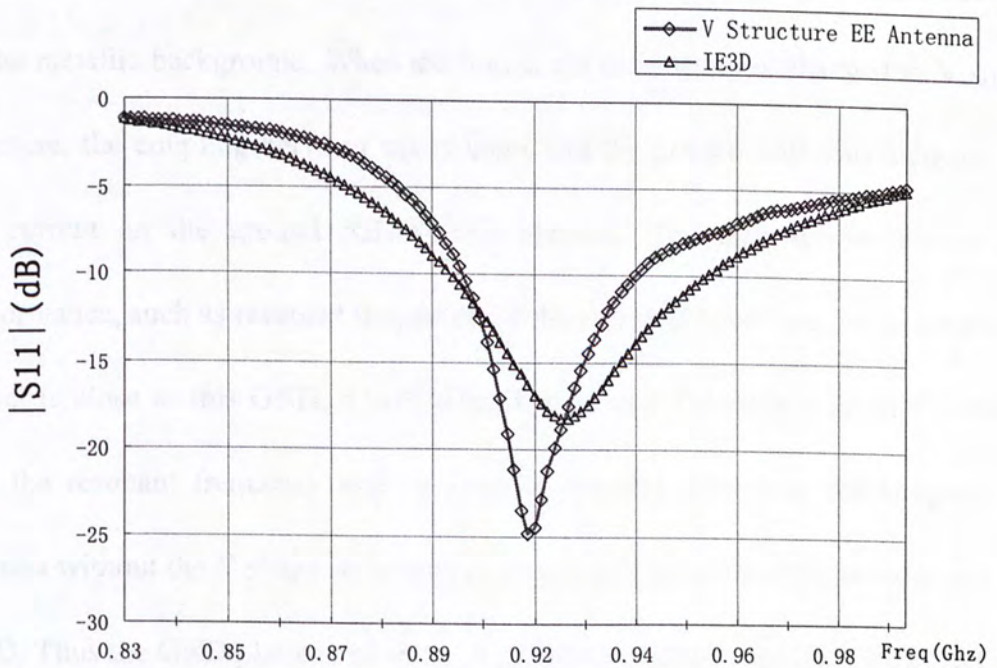


Figure 4.6.8 Comparison Result between Simulation and Experiment

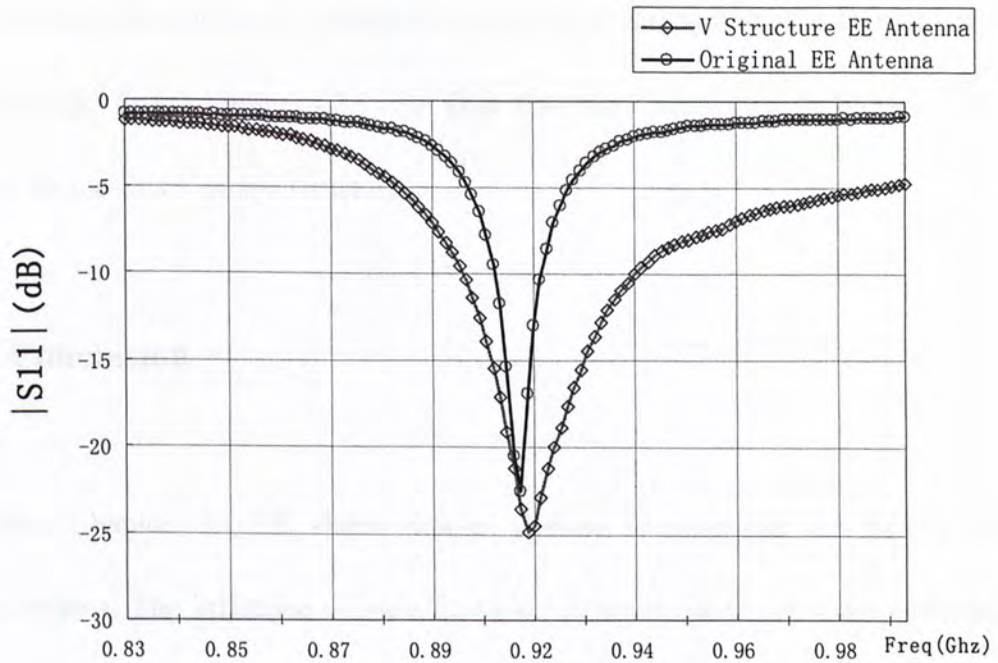


Figure 4.6.9 Comparison between Original EE Antenna and a V Structure EE antenna

From Figure 4.6.6 we note that the resonance frequency is slightly changed because of the metallic background. When the horizontal main trunk is changed to V shape structure, the coupling between the radiator and the ground will also increase. So the current on the ground (GND) will increase. The current also affects the performance, such as resonant frequency, of the antenna. Therefore, when a metallic object is close to this GND, it will affect the current distribution on this GND so that the resonant frequency will be slightly changed. However, the Original EE antenna without the V shape structure has less coupling between the radiator and the GND. Thus the GND plane is working as a partition between the metallic object and the radiator. This is the reason why the original one is not affected by the metallic object whereas the V shape structure antenna is more sensitive to the metallic background. Although there is a shift of the resonant frequency, the antenna

bandwidth still covers the operating bandwidth of our system due to its improved bandwidth. From Figure 4.6.9 we find that the bandwidth is increased a lot according to this V shape structure.

4.7 Conclusion

In this Chapter, an EE shape dipole antenna is proposed for Active RFID applications. The influence of metallic object is investigated for some applications are related to metallic objects such as a container yard management. From the simulation and measurement results we note that the EE antenna will not be affected by the metallic background. The maximum antenna gain is around 5dBi. The measured -10dB bandwidth is around 12MHz. The bandwidth already covers the requirement bandwidth. The operating principle is also investigated in this chapter. Using the lossy transmission line model a reasonable S parameter is attained. The validity of this lossy transmission line model is verified by comparing the S parameter obtained by the Lossy TLN model and the EM simulation by IE3D.

A V shape structure is proposed for increasing the bandwidth of the EE antenna. With this V shape feeding structure, the bandwidth gets a significant improvement. The size of the EE antenna can also be reduced by increasing the capacitive pad size of the supporter. The input impedance can be easily matched by moving the feeding position along the main trunk of the antenna.

Reference

- [1] *Performance Specification for Radio Frequency Identification Equipment (RFID) Operating in the 865-868 MHz and/or 920-925 MHz Bands*
- [2] *ISO18000-7*
- [3] Lora Schulwitz “*Minimization of Antenna Size for VHF Frequencies*”
- [4] Dvid K,Cheng “*Field and Wave Electromagnetic*” Addison Wesley, 1983
Chapter 11
- [5] Dvid K,Cheng “*Field and Wave Electromagnetic*” Addison Wesley 1983
Chapter 9
- [6] CONSTANTINE A. Balanis, “*Antenna Theory*” John Wiley & Sons, INC 1997,
Chapter9, P477.
- [7] Dvid K,Cheng “*Field and Wave Electromagnetic*” Addison Wesley, 1983
Chapter 7. P342
- [8] William F. Richards, Yuen T. Lo “An Improved Theory for Microstrip Antenna and Applications” *IEEE Trans. Antennas Propagation*, Vol. AP-29, No.1, Jan 1981
- [9] J.R. James, “*Microstrip antenna: Theory and Design*” Peregrinus on behalf of the Institution of Electrical Engineers, 1981

Chapter

5

Conclusion

An Active RFID system is implemented for container yard management in this dissertation. This Active RFID system has the capability to collect Tag IDs and read or write tags under LOS or NLOS situations. Eventually the measurement result achieves our design aims. The communication distance is more than 100 meters with a 5dBm output EIRP.

To save more power and avoid interference, a novel wake up strategy is proposed in Chapter 3. A single tone sub-carrier wake up signal is changed to a modulated signal with time marker information in this new wake up strategy. From experiment results we know that this new wake up strategy saves large amounts of power, especially in container yard management, when compared with the old wake up strategy. The modulated wake up signal also has an anti-interference effect. As we already discuss in Chapter 3, a fake wake up signal can be distinguished from a true wake up signal because of the modulated character. Therefore, this modulated wake up signal can help tags to save significant power and also prevent tags being wakened up by a strong interference.

A novel EE antenna is also proposed in this dissertation. Simulation results and measurement results show that this kind of antenna almost does not be affected by a metallic background. A lossy transmission line model is proposed for explaining the working mechanism of the antenna. From the S parameter comparison between the lossy TLN model and IE3D model we find that these two models match well. Thus we consider this lossy TLN model as a proper model to describe the antenna. A V shape structure is proposed to increase the bandwidth of the antenna. From the measurement and simulation results we note that the bandwidth gets a significant improvement.

CUHK Libraries



004359185